CO_2 Foam for Heavy Oil Recovery: Stabilization of CO_2 Foam by Nanoparticle and Polymer

by

Daimeng Jia

A thesis submitted in partial fulfillment of the requirements for the degree of

Master of Science

in
Petroleum Engineering

Department of Civil and Environmental Engineering
University of Alberta

ABSTRACT

Due to unsatisfactory sweep efficiency of gas injection, foams, CO_2 foams in particular, are utilized to reduce residual oil saturation. Conventionally, generation and stabilization of CO_2 foams are achieved by surfactants. However, foams, stabilized via this traditional method, tend to sustain undesirable stability with relatively short term under reservoir conditions. Because of their outstanding stability, nanoparticles can be used to mitigate such weakness. Moreover, a viscosifying polymer is used along with surfactant and nanoparticle to stabilize the foam. However, the challenge is to understand how the combination of surfactant, polymer, and nanoparticles improve the performance of conventional foam for heavy oil recovery.

In this thesis, a new type of foam generated with Surfactant, Polymer, and Nanoparticle (SPN foam) is used to access the trapped heavy oil. SPN is employed to stabilize CO_2 foam and mobilize unrecovered heavy oil, and its performances are compared with scenarios in the absence of nanoparticles. Surface functionalized silica Nanoparticles was used to investigate the performance on foam stability. A visual linear sand pack was used to study the foam performance during heavy oil recovery. Foams are formed in situ by co-injection of the foaming solution and CO_2 gas. In static tests, the decreasing rate of foam height and foam half-life are recorded and described as foam stability. A high-quality digital camera is employed to capture images of the related phenomenon.

Results reveal that the surfactant-nanoparticle-polymer foam is superior to conventional

approaches in terms of foam static and dynamic stability, which indicates synergy between surfactant and nanoparticles. Nanoparticles mainly involved in the liquid-gas interface and increase the foam stability and foamability. The addition of polymer enhances the liquid viscosity and foam stability in static tests. Moreover, foam stability is improved more obviously in the presence of crude oil. Successful foam generation and escalation were achieved in water-saturated dynamic experiment after introducing nanoparticle and polymer into the surfactant dispersion. In terms of dynamic tests in the presence of oil, foam flooding of surfactant-nanoparticle-polymer blend obtained the most desirable pressure drops and oil recovery. The synergism between nanoparticle and surfactant apparently enhanced the foam propagations and polymer has a positive impact on foam performances.

The application of nanoparticles stabilized foam for heavy oil recovery has several advantages. Besides enhancing the foam stability and foamability, the presence of nanoparticles mitigates the amount of surfactant used for foam generation.

My work is dedicated to

My husband, parents, and grandma

For their endless love, support, and encouragements

Which illumine my life.

ACKNOWLEDGEMENTS

It is my pleasure to write the acknowledgements since I had enjoyed great benefits of valuable supports from people around me during my graduate study. Now it is the time to express my appreciations to all these awesome people.

I would like first to thank my supervisor Dr. Japan Trivedi for his supervision, motivations, and patience throughout my master period. I am grateful to Dr. Trivedi who offered me the opportunity to study and research at the University of Alberta and provided me effective supports allowed me to overcome any difficulties and accomplish my study successfully. I am grateful to Dr. Hassan Dehghanpour and Dr. Rajender Gupta for serving as members of my examination committee and providing valuable feedbacks.

I would extend my thanks to all my colleagues in our team for sharing their ideas during each group meeting and assisting me in my experiments whenever needed. It was an honor to work with all the group members. I would like to express my thank especially to Ali Telmadarreie, who was always willing to afford me help and advice regarding on my research directions and experimental setups.

I am thankful to our technologist, Todd Kinnee, for his continuous technical support.

Last but not least, I gratefully acknowledged to my family and all my friends who offered me spiritual supports, courage, and inspiration during my graduate study. Without them, I could not achieve my dream unhesitatingly.

TABLE OF CONTENTS

LIST OF TABLES

LIST OF FIGURES

Chapter 1: Introduction

1.1 Introduction

From early research and successful attempts to a widely known and practiced enhanced oil recovery (EOR) technique, the CO_2 gas flooding has been used for more than six decades. Chemically stable nature and economically accessible both through natural and anthropogenic sources contribute to the advantages of applying CO_2 as gas flooding ingredient (Mungan, 1981). The CO_2 gas flooding is also less environmentally harmful by reducing anthropogenic carbon released to the atmosphere since a significant amount of CO_2 is required to be injected into the reservoir (Malik and Islam, 2000). However, CO_2 gas flooding EOR has a critical weakness of poor sweep efficiency, which is caused by viscous instability, gravity segregation and reservoir heterogeneity (Rossen et al., 2010). High mobility nature of gas creates fingering or channeling situation in the reservoir, particularly when the porous media has a high permeability (Koval, 1963). Even more complicated reservoir situation occurs when density differentiate significantly between oleic and gaseous matters caused by gravity segregation (Eftekhari and Farajzadeh, 2015; Lake et al., 2014). In order to control flooding mobility, CO_2 foam is employed.

1.2 Background

In last two decades, foam has been proven to be the most anticipated method for enhanced oil recovery and still is the most efficient approach for reservoir flooding (Rossen et al., 2010). Depends on the type of geological settings foam formed in situ may perform differently. Generally, the dispersion of foam can remarkably reduce the gas permeability

of porous media hence increase the gas sweep efficiency which means a greater amount of crude oil can be propagated out of the reservoir as the foam sweeps through porous media. However, the longevity can be an issue of this approach due to the thermodynamically unstable nature of foams. Although by continuously adding foam to gas injection stream can maintain the level of foam in a reservoir (Bernard and Holm, 1964), still more economically feasible technique is needed.

To increase recovery efficiency foams formed in situ was aimed to magnify the flexibility of fluid transportation in a porous medium. Colloidal particles that implemented to generate foams were not only tested for emulsifying intensity but also the stability of foams. Considering the accessibility and affordability of all foaming agents, surfactant became a major player in the oil and gas industry in 90's. The amphiphilic nature of surfactant particles provides significant stability for foam by forming protective layers between the substances. Molecular wise a surfactant particle will submerge its hydrophilic head into the liquid and tail its hydrophobic side along the gas upon contact with reservoir mediums (Eftekhari and Farajzadeh, 2015). One of the many advantages of using a surfactant in EOR process is the maneuverability of anthropogenic production. Depends on the reservoir's circumstance, the surfactant can be utilized to either forming foams to conserve the gas phase or liquid phase. The degree of polarization of different surfactant particles affects the extent of surfactant dissolution into liquids. Also, the difference of contact angles between water/oil or water/air interface will cause surfactant particles to bulge either along the aqueous surface or away from it (Espinosa et al., 2010). However, during the surfactant propagations in the reservoir, a significant amount of particles would be wast-

ed due to indiscriminate attachment (Grigg and Mikhalin, 2007). Partitioning between oils and surface adsorption from the bedrocks severely decreased the economic efficiency in subsurface usage of surfactant (Singh and Mohanty, 2014).

Statement of Objective

The objective of the thesis is to investigate the performance of CO_2 foam stabilized by a blend of surfactant, nanoparticles, and polymer in the presence and absence of heavy oil. Static tests were performed to study the foam stability and foamability by analyzing the decay of normalized foam height over time and initial foam heights. A visual linear sand pack was utilized to conduct the dynamic experiments in water-saturated and oil-saturated conditions. The foam was generated in-suit by co-injecting foaming dispersions and CO_2 gas with a fixed foam quality. Pressure drops during the foam injection were monitored, and oil recovery in the presence of oil sand pack was recorded. To investigate the effect of nanoparticles and polymer additions on foam behaviors, the same experiments procedures were conducted in environments of surfactant sole, surfactant-nanoparticles, and surfactant-nanoparticles-polymer, respectively.

Chapter 2: Literature Review

Nanoparticles stabilized foam tends to exhibit long-term stability compared with foam generated by surfactants. According to Nguyen et al. (2014), coated silica nanoparticles and SDS (sodium dodecyl sulfate) surfactant were used to stabilize CO_2 foam in same conditions, and results revealed that foam created by nanoparticles was dramatically more stable. Worthen et al. (2013) announced that proper nanoparticles were able to stable air foam for more than a week.

The ability to stabilize foam at relatively low concentrations contributes to another advantage of nanoparticles. Yu et al. (2012) pinpointed that 4000-6000 ppm of silica nanoparticle could establish stable CO_2 foam. Espinosa et al. (2010) illustrated that 0.05 wt. % of surfaced modified nanoparticles can generate foam with long-lasting character.

Moreover, nanoparticles tend to be more attractive due to low cost. Researchers demonstrated that nanoparticles could be formed by modifying low-priced materials such as silica or even fly ash (Singh and Mohanty, 2014; Paul et al., 2007). The fly ash which defined as any non-combustible inorganic solid materials that usually in size of micrometers is a by-product of coal combustion. Normally treated as a waste during energy generation process, fly ash can be obtained in great quantity at low economical value. Potentially to convert mirco-sized fly ash into nano-sized particle is also economically efficient by using grinding and de-agglomeration techniques (Eftekhari and Farajzadeh, 2015). And sufficient core flooding experiments had suggested that tertiary oil recovery was enhanced by nanoparticles stabilized foam due to its high stability (Mo et al., 2014; Worthen et al. 2013).

2.1 Nanoparticle-stabilized emulsions/Foams

The use of nanoparticle instead of surfactants to achieve superior stable foam is the frontier of research. Nanoparticle was recently introduced to petroleum industry due to the rapid development of nanotechnology. Since it became economically efficient and can be commercially manufactured, the usage of nanoparticles was magnified in the industry. It has the advantages of standardized sizes also available in any surface properties. Nanoparticle's surface properties also termed as wettability is fundamentally the shape of solid particles which can be altered and manufactured in uniformity. By adjusting the nanoparticle's configuration more stable foams with better performed surface properties can be produced. Furthermore, nanoparticle can survive better than surfactant under high temperature and high salinity environment (Zhang et al., 2011; Bragg and Varadaraj 2003). A Pickering emulsion which is equivalent to colloidal particles stabilized emulsifying process tends to stabilize in situ generated foams. Nanoparticle stabilized emulsion is more resilient towards reservoir environment than surfactant stabilized emulsion also tends to last longer period of time (Zhang et al., 2011). In term of emulsion mechanism (Binks 2002; Eftekhari and Farajzadeh, 2015 and Worthen et al. 2012) has implied: when solid particle is used as emulsifying agents, it can be attached on the gas-liquid interface. In fact the involvement of nanoparticle signified the emulsifying process by forming stable foams. If nanoparticles entered into gas-liquid interface in a favorable angle, the adsorption energy will be high enough to cause the process irreversible. The adsorption energy for spherical particles on gas-liquid interface is calculated by

$$E = \pi r^2 \sigma_{gw}(1 \pm cos\theta)^2$$

where r is defined as the radius of a particle and σ_{gw} is the gas-liquid interfacial tension. Where θ is the contact angle that particle measured into the liquid phase or aqueous phase.

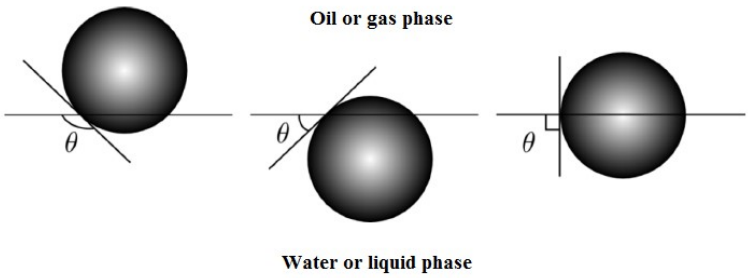

Figure 2.1.1 - θ the contact angle of nanoparticles at gas-liquid or oil-water interface (Binks 2002; Eftekhari and Farajzadeh, 2015)

The contact angle θ is critical in term of defining the spherical particle is hydrophobic or hydrophilic. When particle is hydrophobic, area of its surface submerged in the aqueous phase is smaller than the area exposed to air or oil and the contact angle is greater than 90 degree. Whereas particle is hydrophilic, portion of the particle's surface left in air or oil is less than that in the water and θ is less than 90 degree. Then consider forming monolayers with spherical nanoparticles, such layers will arc towards the side of less exposed surface of each particles. (Fig. 2.1.2)

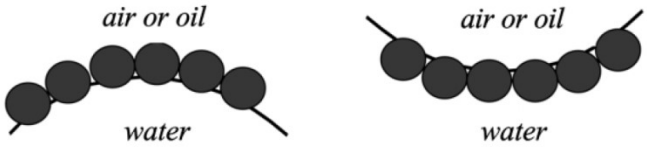

Figure 2.1.2 - Arced fluid-water interface formed by hydrophilic particles and hydrophobic particles. (Binks, 2002)

The last component that effects stabilization of foam is detachment energy. Greater the energy for a spherical particle to detach from the fluid-water interface, harder the particle formed foam tends to deform. Thus particles with the significantly reduced size i.e. nanoparticle, the energy that required to remove it from fluid-water interface are so high, which cause the adsorption nearly irreversible. For instance, a particle with a diameter of 20 nm, which is the diameter of the nanoparticle from Nyacol, enters the interface at θ is 90 degree will have detachment (adsorption) energy around 20,000 kT.

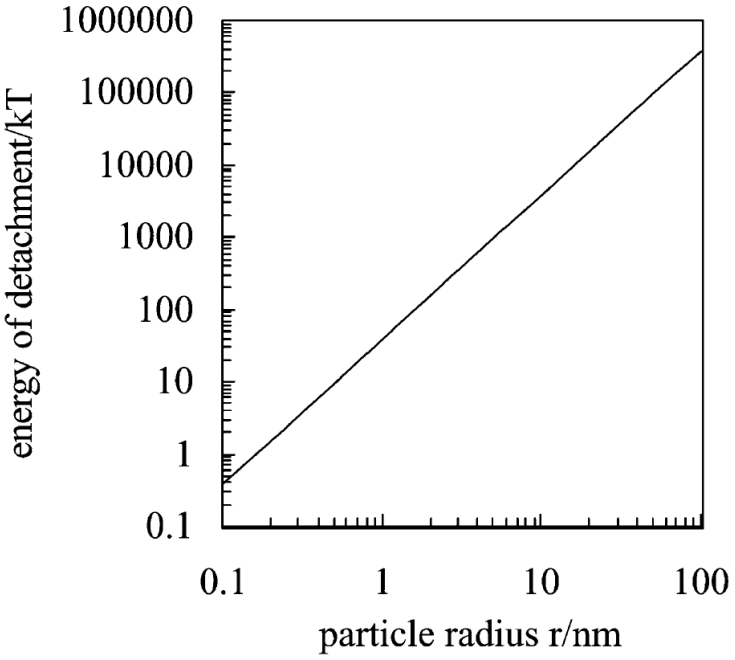

Figure 2.1.3 - Energy for single spherical particle to detach a planar oil-water interface, interfacial tension 50 mN m^{-1} with contact angle of 90 degrees versus particle radius at ambient temperature 298 K. (Binks, 2002)

However, when the contact angle is either above 150 degrees or below 30 degrees, hydrophobic and hydrophilic particle respectively, the detachment energy would be very low so any stable foam cannot be generated (Singh and Mohanty, 2014). The nanoparticle is capable of stabilizing emulsion better than a surfactant. In 2004, Dickson et al. had proved that nanoparticles could better-stabilized CO_2 in water emulsion than a surfactant. Surfactant emulsified CO_2 is less stabilized because the molecular structure of CO_2 lacks a permanent dipole moment and CO_2's weak van der Waals forces, thus surfactant attached CO_2 tails are indisposed solvated (Espinosa et al., 2010).

2.2 Nanoparticles Transport

In term of the transportation, nanoparticles have unparalleled advantages in size. It has been found in a study that porous media can trap particles that travel through them, from pore throats and absorbing particles onto the rock surface (McDowell-Boyer et al., 1986). The size exclusion mechanism of pore throats is out of discussion due to the nanoparticle is significantly smaller than the normal pore throats. Nonetheless, the surface retention force of porous media potentially has a negative impact on the distance that nanoparticles travel. However, in 2009 and 2010, two groups of researchers (Rodriguez et al. and Caldelas, respectively) had done experiments regarding the retention capabilities of the surface of sandstone towards nanoparticles and the results are not disappointing. In the former experiment, researchers flush total sizes from 10 nm to 25 nm PEG coated silica nanoparticles provided by 3M® Company through limestone and sandstone cores, the amount of nanoparticles that is retained ranges from 2% to 12%. As well as in the latter study, the retention rate is no greater than 10% for 20 nm no surfactant coated silica nanoparticles and PEG coated silica nanoparticles flushing through consolidated sandstone and limestone cores and unconsolidated sand pack columns. Both studies had reinforced the capability of transporting nanoparticles in the reservoir. Furthermore, nanoparticles have another advantage comparing with surfactants. In 2012, Zhou et al. had found the amount of surfactants adsorbed by reservoir rocks increase as the distance of transportation increase. Eventually, a film of surfactants was absorbed onto the rock and thus diluting the injected solution as surfactant moves further in porous media. Although the study showed the amount of surfactant adsorption is a lot lower at second than the first injection, it still mentioned potential economic ineffectiveness for using a surfactant as a

foaming agent (Zhou et al., 2012). However, nanoparticles can move through porous media, independent of lithology, at much less retention rate (Zhou et al., 2012; Gabel, 2014).

2.3 Surface modified nanoparticles

As an effective foaming agent, nanoparticles can be used solely in applications (Binks and Horozov 2005). Bare and unmodified nanoparticles are not used as emulsifying reagent since unmodified silica particles' hydrophilic behavior will cause dissolution. It has been found by Davidson in 2012 that coated nanoparticles which contain a core made of iron oxide can generate heat when placed into a local induced magnetic field. Thus potentially the materials that nanoparticles made of can be propagated so that desired functional properties can be obtained and utilized. Also, surface modifications to nanoparticles can give them catalytic or reactive properties (Zhang et al. 2009).

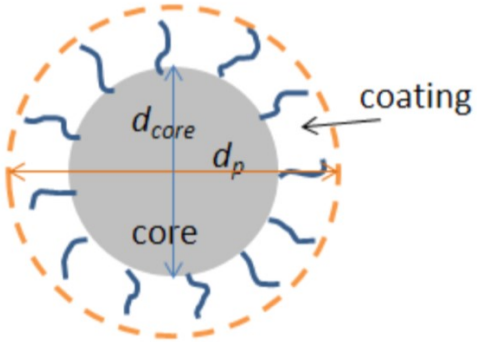

Figure 2.3.1 is a schematic of a surface coated nanoparticle. (Gabel, 2014)

In 2010, Zhang et.al. had studied intensely over the subject of nanoparticle-stabilized emulsions which had used the diameter of 10 nm polyethylene glycol (PEG) coated silica nanosphere. The PEG coated nanoparticle which produced by 3M Co., St. Paul. MN. was

tested for phase behavior when forming an oil in water emulsion. While factors such as particle structure, rheology of particle concentration, salinity, and initial volume ratio were taken into consideration, PEG coated silica still performed significant capability in term of forming an efficient and stable emulsion. One of the highlights of PEG coated nanoparticle is that the amount of oil been emulsified from water phase is much higher in term of volume fraction. When the nanoparticle concentration was controlled 0.5wt% or higher (up to 5wt% in the experiment) and salinity varies from 0 to 10% of the bulk emulsion, the volume fraction of oil to water was stabilized at around 0.7 with no obvious deformation.

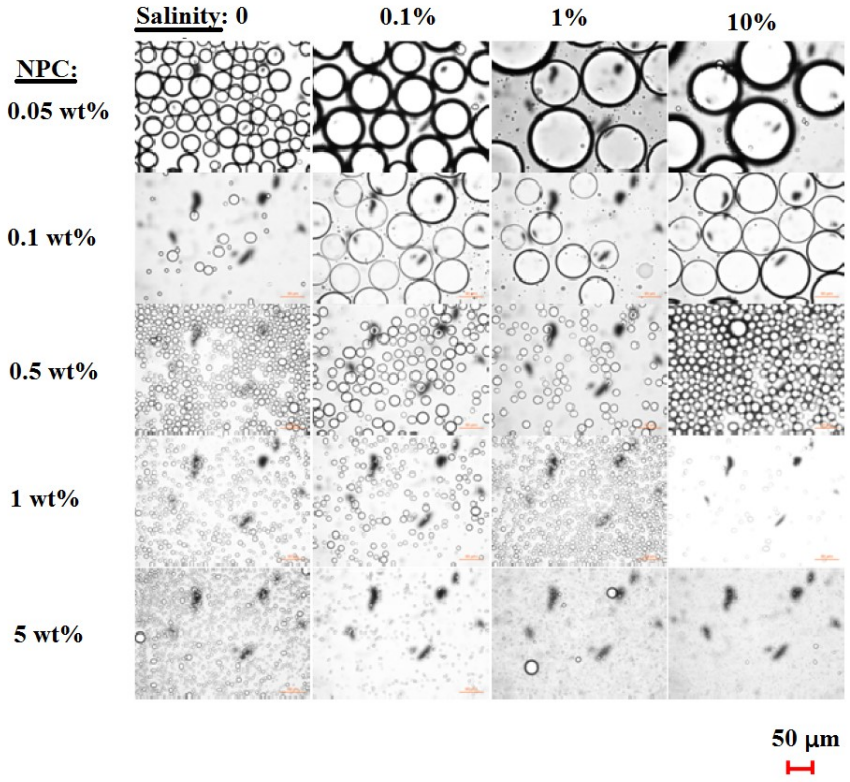

Figure 2.3.2 - Pictures of oil droplets in the oil-in-water emulsion. Salinity increase by weight percentage from left to right; NPC – nanoparticle concentration increase from top to bottom, with initial volume ratio: oil/water equals to 1. (Zhang et al., 2010)

Another kind of surface modified silica nanoparticle that been experimented intensely is fumed silica nanoparticle. By controlling the amount of dichlorodimethylsilane been modified onto the surface of silica particles, stabilized O/W emulsion is achieved (Binks and Lumsdon 2000; Binks and Horozov 2005). However, the process of wetting fumed silica nanoparticles in water is complicated and inefficient due to its hydrophobic nature. First, the silica solids have to be wetted with alcohol, then centrifuging the solution, then removal of the alcohol solvent and finally re-dispersed the silica particles into water. Also, the removal of alcohol solvent alone has to be repeated multiple times to minimize any presence of unwanted alcohol. Worthen et, al. (2012) and Nguyen et, al. (2014) had implemented this method to wet 50 percent dichlorodimethylsilane (DCDMS) coated silica particle, provided by Wacker-Chemie, with less than 1% v/v of unwanted alcohol in solution. The method was also used by Binks and Horozov (2005) for wetting different grades of DCDMS (0~86%) coated silica particles, provided by Wacker-Chemie as well, with less than 10^{-4}wt% residual ethanol.

2.4 Nanoparticle and surfactant stabilized foam

Although nanoparticle can stabilize foam solely, mixtures of nanoparticles and surfactants are found to be more efficient regarding foam generation, because the two stabilizers can act synergistically to achieve superior stable foam (Binks et al., 2007; Binks et al., 2007). Emrani et al. (2015) investigated the effect of nanoparticles in the establishment of CO_2 foam in AOS (alpha olefin sulfonate) surfactant dispersions and observed that the foam stability was boosted even at low concentration of nanoparticles (0.1 wt.%). Binks et al. (2008) utilized silica nanoparticles and di-C_{10}DMAB (di-

decyldimethylammonium bromide) to study the synergism between the two foaming agents. Adsorption of surfactants onto nanoparticles surfaces was recognized, suggesting synergism appeared. Significant improvement in foam stability was noted when foam was generated by surfactant-nanoparticles blend instead of a sole foam stabilizer. The long-term foam stability tends to have a positive impact on oil recovery. Singh and Mohanty (2014) emphasized that foam formed by a mixture of surfactants and nanoparticles enhance the tertiary oil recovery by approximate 10% of the original oil in place. The synergistic interactions between the reagents are one of the factors that contribute to the mixture of surface-modified nanoparticles and surfactant being stable. Anionic surfactant has electrostatic interactions with positively charged nanoparticle surfaces results in a more resilient monolayer formed at water particle interface (Singh and Mohanty, 2014).

2.5 Mobility control (polymer)

Polymers are extensively used in field operations to ultimate the efficiency of heavy oil displacements. Compared with conventional foam, the polymer-thickened foam had favorable performance in the presence of heavy oil (Telmadarreie and Trivedi, 2016). In the applications of polymer enhanced foam, the polymer can increase the viscosity of chemical solutions, resulting in improvements in both foam viscosity and stability (Sydansk, 1994). Telmadarreie and Trivedi (2016) illustrated that polymer addition could abate the destabilizing effect on foam stability caused by oil. Among various types of polymers, polyacrylamide is employed as a mobility control agent because it is relatively inexpensive to produce and its chemically stable nature (Thomas et al., 2012). Schramm and Kutay (2000) clarified the viscosity of surfactant-stabilized foam was remarkably

intensified after adding a small amount of polyacrylamide. Alargova et al. (2004) had found that rod-shaped polymer in length of tens of micrometers can stabilize foams in a week with minimal change of foam volume (foam stayed constant volume at 1.3mL). The polymer particles achieve longer foaming stability due to the entangled outer layers of bubbles that protected the bubble from deformation. The superstabilization of foam by these polymer microrods had illustrated the significant advantage of polymer stabilized foam over conventional surfactant as a foaming agent in term of magnificent longer in foam lifetime. Espinosa et al. (2010) demonstrated polyethylene glycol coated silica nanoparticles' capability of stabilizing carbon dioxide foam generation by simulated foam generate pressurized reservoir environment in compacted columns. During the experiment, nanoparticle-stabilized foam kept its stability well under theoretically undesired environment when the nanoparticles remain dispersed in the water phase (Singh and Mohanty, 2014).

Chapter 3: Experimental Methodology

3.1 Materials

Surfactant: Cationic surfactant Cetyltrimethyl Ammonium Bromide ($C_{19}H_{42}NBr$), CTAB, was purchased from BioWorld in a dry powder form with a purity of greater than 99.0% and molecular weight of 364.45 g/mol.

Nanoparticles: The nanoparticles used in this paper were colloidal silica nanoparticles Nyacol DP9711 (Nyacol Nano Technologies, Inc), received as a 30 wt. % aqueous dispersion. These nanoparticles are surface modified (believed to have polyethylene glycol coating, which enables this nanoparticle to be hydrophilic (Roberts, 2011; Singh and Mohanty, 2014) with an average particle size of 20 nm. With excellent stability, these nanoparticles tend not to be agglomerate even in high salinity and pH environments.

Polymer: The non-ionic and water soluble polymer, polyacrylamide, was obtained from Acros Organics with approximate molecular weight of approx. M.W. 5 to 6.000.000.

Crude Oil: The heavy crude oil used for both of the static and dynamic experiments was collected from a Canadian oilfield with dead oil viscosities of 1300 cp and 600 cp, respectively (viscosities were measured at 22 °C).

Carbon Dioxide Gas: Carbon Dioxide utilized during in-suit foam generation was purchased from Praxair Co.

Other materials: Brine with 0.1wt% of Sodium Chloride (NaCl) was used for water saturation and water flooding in dynamic experiments. Deionized (DI) water, purified from tap water, was utilized in all experiments.

3.2 Apparatus

3.2.1 Experimental set-up for Static tests

Homogenizers

Polytron® PT 6100 D Homogenizers was used to generate foam, which was purchased from Kinematica Inc. The homogenizer is equipped a motor of 1700 Watt, which provides sufficient power to enable speed to achieve high values (from 500 to 30, 000 rpm). During our experiments, the speed was set to be 7,000 rpm and the mixing duration was maintained for two minutes to ensure foam was created desirably. Figure 3.2.1 showed the exterior of the homogenizer.

Figure 3.2.1: Homogenizer (Polytron PT 6100 D)

3.2.2 Experimental set-up for Dynamic Tests

The core flooding set-up was designed to create in-situ foam, which was illustrated schematically in Figure 3.2.2. To enable in-situ foam generation and flooding, foaming solutions and carbon dioxide gas was injected simultaneously into the visual cell, which was initially packed with silica sands and then saturated with liquid phases (brine only or brine followed by crude oil) depending on experiment conditions. All the experiments were conducted at the ambient temperature. The set-up consisted of apparatus including three accumulators filled with brine, crude oil, and foaming dispersions, a visual sand pack, a ISCO pump, a gas cylinder where carbon dioxide gas stored, a mass flow controller (MFC), a pressure transducer, and a graduate cylinder, which was used to collect produced mixtures. A camera was utilized to capture images of the visual sand pack during foam flooding durations, and a computer worked together with the mass flow controller and pressure transducers to recode experimental data. The details of apparatus were demonstrated in the following sections.

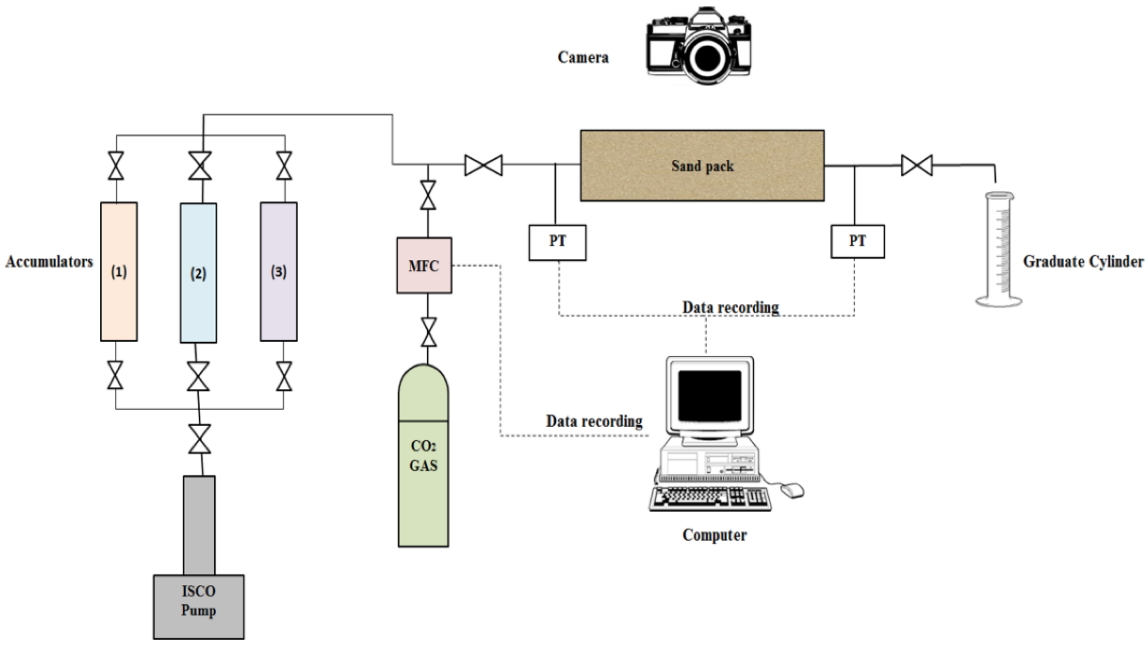

Figure 3.2.2: Experimental setup for foam flooding: the accumulator (1) contained brine; the accumulator (2) contained crude oil; the accumulator (3) contained foaming dispersions; MFC: mass flow controller; PT: pressure transducers

Sand pack

Silica sands (100-170 meshes) were packed into a visual sand pack, which was cylindrical in size with a length of 1 ft and an internal diameter of 1 inch. To induce mixing and settling of artificial sands, continuously shaking of the dry and cleaned sand pack was required during the packing process. The glass column was sealed via a metal screen and followed by an expansible rubber stopper at each end. Figure 3.2.3. illustrated the visual sand pack, metal screens, two ends with expansible rubble stoppers, and all the connections including valves.

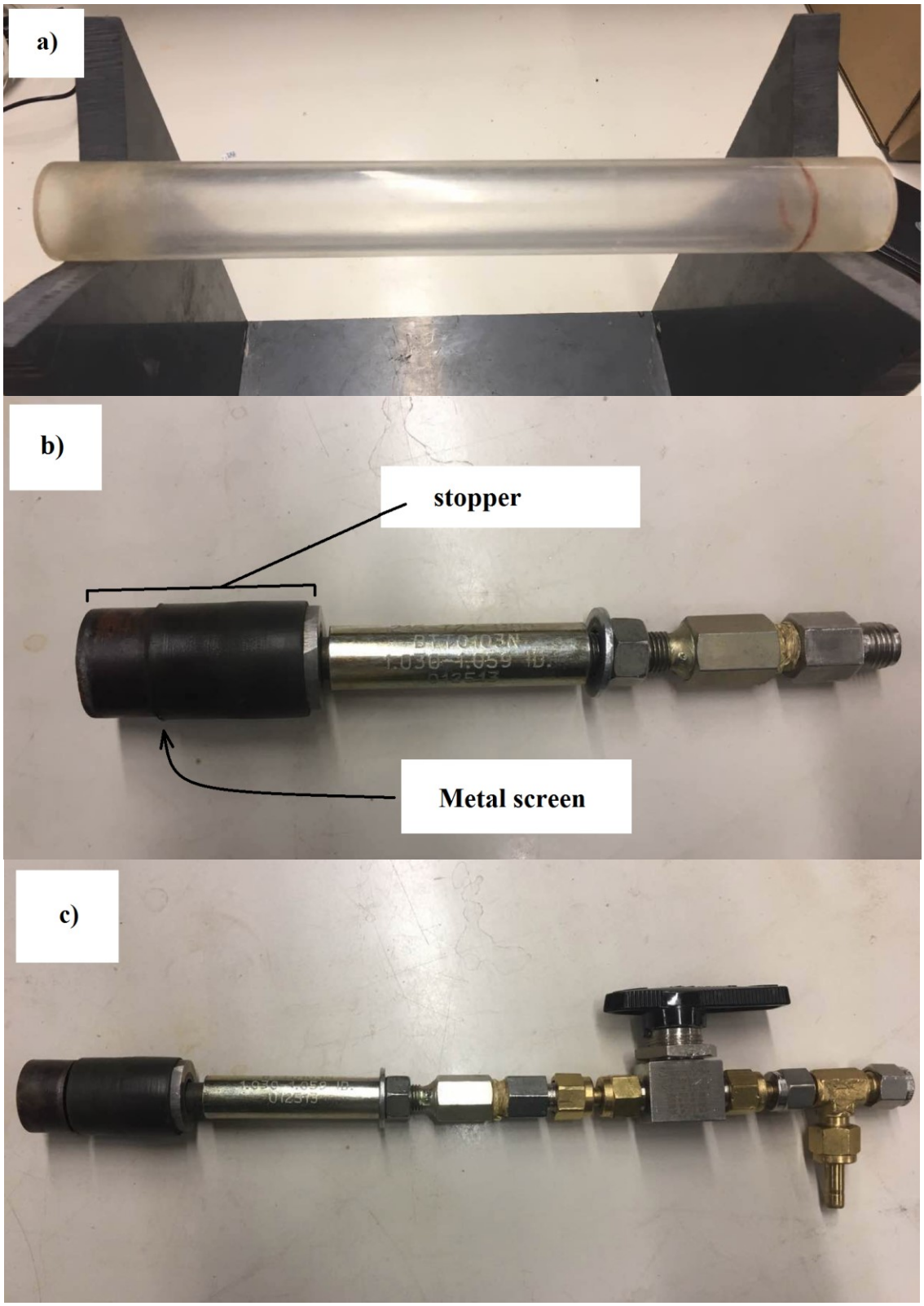
a)
b)
stopper
Metal screen
c)

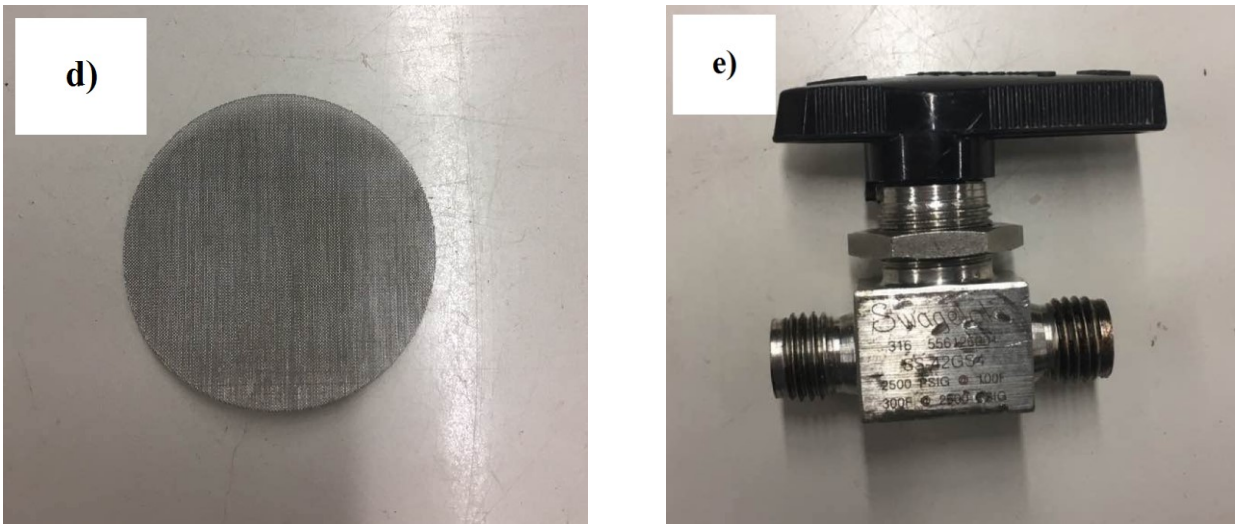

Figure 3.2.3: (a) the visual sand pack; (b) and (c) two ends with expansible rubble stoppers and connections; (d) the metal screen; (e) a two-way valve

Pumps

A syringe pump (model 500D) was purchased from Teledyne ISCO Inc.. It was utilized to work together with accumulators to inject liquids into the visual sand pack to allow foam flooding. The syringe pump was filled with water initially and then connected with one of the accumulators. While operation, the pump water was displaced by liquid phases (brine, crude oil, or foaming solutions), which were stored in accumulators previously. The pump has a capacity 500 cc. It can be used functionally up to a pressure of 3,750 psi, which fully covers the experimental pressure conditions. The liquid flow rates can be adjusted from 0.001 to 204 cc/min, and we set the flow rate to be 30 cc/min when conducting experiments. Since experiments were performed at the ambient temperature, it met the temperature restriction of the pump which was between 5 to 40 degree Celsius. The flow accuracy of the pump is 0.5% of set point. Figure 3.2.4 displayed the exterior of the syringe pump.

Figure 1Figure 3.2.4 The Syringe Pump

Accumulators

Three accumulators in total were applied in dynamic experiments, with proper sealing, the accumulators had a floating piston inside, which functioned as a separating element. By connecting one end of the accumulator with the syringe pump and the other end with the visual cell, the pump water was injected into the accumulator and lifted the piston upward to push pre-stored solutions or crude oil into the visual sand pack. By such displacement process, it could avoid directly filling the pump with chemical dispersions,

which may cause corrosions or cleanliness issues, especially when nanoparticles, surfactants, polymers, brine, and crude oil were involved in operations. The three accumulators were employed in different stages of core flooding experiments: the accumulator (1) which contained brine was used in water saturation and water flooding; the accumulator (2) which contained crude oil was utilized in oil saturation; and the accumulator (3) which contained foaming solutions was used in foaming dispersions pre-flush and foam flooding periods. Figure 3.2.5 shown the exterior and interior of the accumulator.

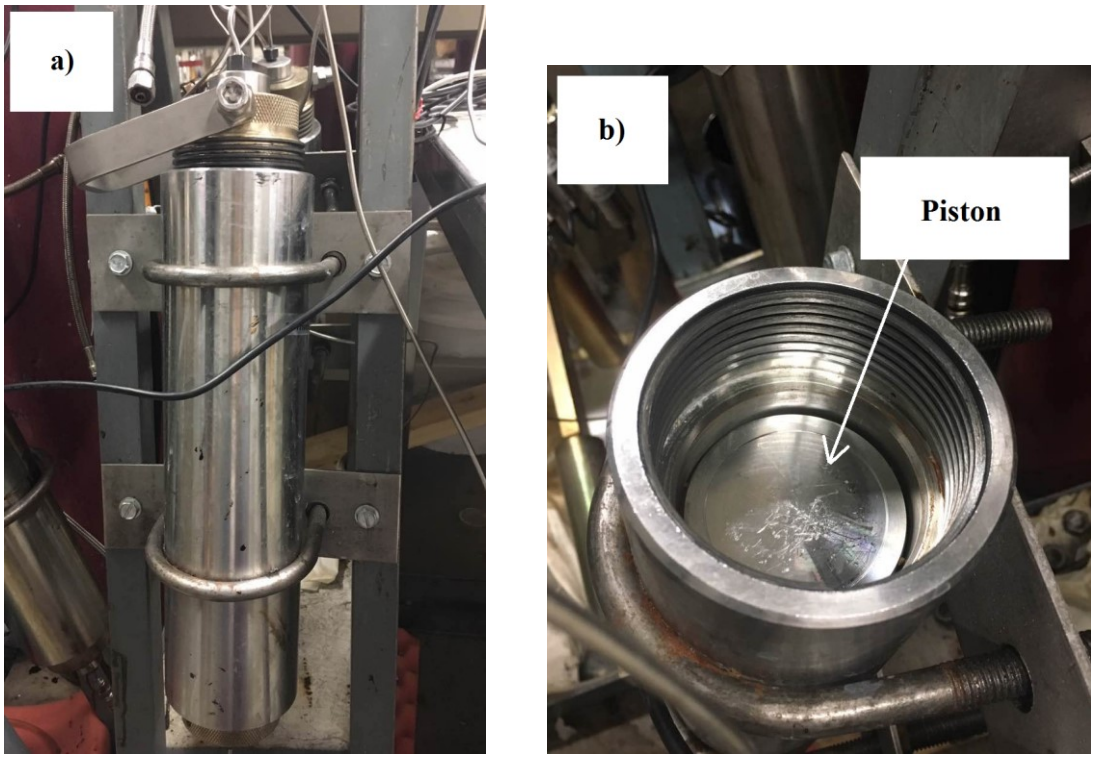

Figure 3.2.5 (a) the exterior of the accumulator; (b) the piston inside the accumulator.

Mass Flow Controller

A gas mass flow controller (Bronkhorst High-Tech) was employed to control gas rate so that the amount of gas that delivered from the carbon dioxide gas cylinder is accurately measured. The mass flow controller is connected to a computer which regulates the gas injection rate also it displays flow rate. The gas flow rate data collected is analyzed by software which was installed previously for functioning the computer with the MFC. Then the desired amount of carbon dioxide gas would be delivered to a sand pack where actual experiment takes place. During dynamic experiments, the injection rate of carbon dioxide gas was set to be 90 ml/h. Figure 3.2.6 displayed the exterior of the mass flow controller and the screenshots of outputs carried out by the corresponding software.

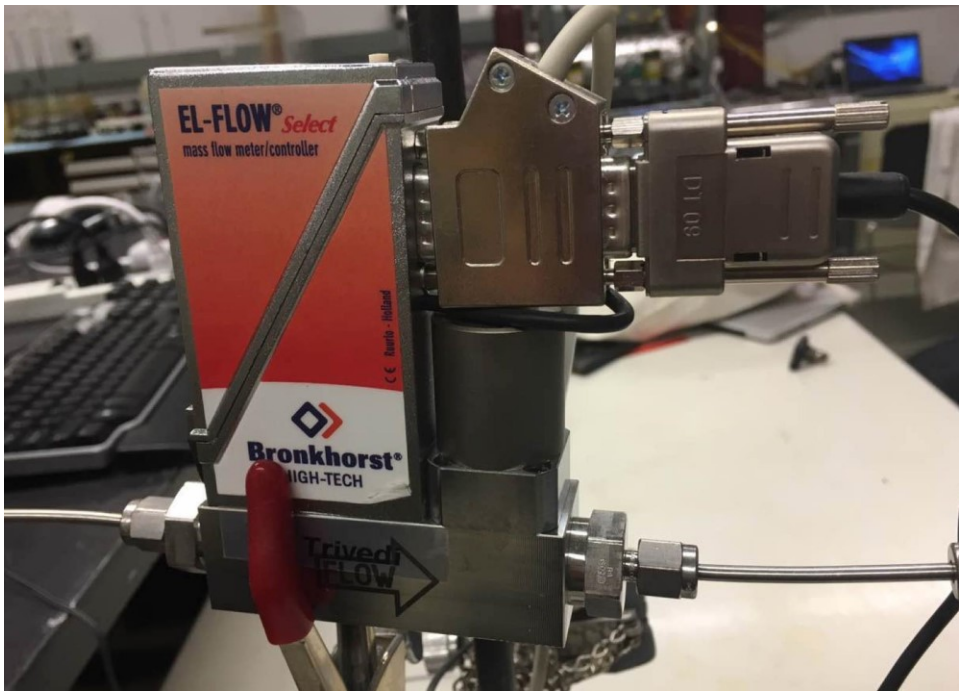

Figure 3.2.6: Mass Flow Controller

Pressure transducer

The pressure transducer was purchased from Omegadyne Inc. with a model name of PX409. After insulating a corresponding software, the transducer can connect to a computer directly. The pressure drops across the sand pack could be monitored and documented. The transducer can obtain up to 1000 readings per second, and the accuracy of those values is ±0.08%. In our experiments, one reading per second was set. The pressure drops measured in experiments were within the range of the transducer (from 0 to 500 psi). Figure 3.2.7 showed the exterior of the transducer: the A end was connected with the sand pack via a T-connection and the B end was linked to a computer to transmit the measured pressure data. Additionally, screenshots were included in the figure as well, which shown the process of the software when it monitored the pressure date and generated a pressure chart versus time

Figure 3.2.7 Pressure transducer (Omegadyne model PX409).

3.3 Procedure

3.3.1 Preparation of Aqueous Dispersions

Three dispersions were prepared using deionized (DI) water, including surfactant only environment, Surfactant-Nanoparticles environment, and Surfactant-Nanoparticles-Polymer environment. The concentrations of surfactant (CTAB), nanoparticles (DP 9711), and polymer (polyacrylamide) were 0.1 wt.%, 1.0 wt.%, and 500 ppm, respectively. The surfactant concentration used in this study was beyond its critical micelle concentration (CMC). All the solutions were in the presence of 0.1 wt.% of sodium chloride. To ensure homogeneous mixing, the dispersions were constantly stirred for 20 hours via a magnetic stirring at a speed of 500 rpm.

3.3.2 Foam Generation

Foam was created via a Polytron® PT 6100 D Homogenizers (Kinematica Inc.). 100 ml of dispersion was filled into a graduated glass cylinder with a capacity of 1000 ml and mixed at 7,000 rpm for two minutes. The foam generation procedures were maintained consistent for the three desperations, specifically for the duration and speed of mixing. In terms of cases in the presence of crude oil, 5 ml of heavy oil was initially added to the solutions before the high-speed mixing.

3.3.3 Static Stability

Due to the significant impact of environmental humidity on foam stability (Li et al., 2012; Sun et al., 2015), the cylinder was always sealed from the top using parafilm immediately after foam generation. In tests involving oil, heavy oil was introduced to the solutions by a syringe before high-speed homogenization. The height of the foam (above the liquid phase) and the position of foam-liquid interface changed over time were

monitored. The foamability can be analyzed based on the original foam height (foam height at time zero). To evaluate the foam stability, the normalized foam height and half-life value were introduced. The uncertainty based on visual measurement of the foam heights was within 0.2 centimeters. Each of the experiment was conducted one more time to ensure the accuracy of the results. All the experiments were carried out at the ambient temperature.

3.3.4 Dynamic Experiment

Before conducting flooding tests, the sand pack model was vacuumed for 20 hours to eliminate air. The dead volume of the experimental setup was calculated in advance to ensure the accuracy of parameters' measurements. With horizontally placed, the sand pack was completely saturated with brine to measure the porosity. Permeability was determined by using Darcy Law.

For dynamic tests in the absence of oil, the core was first flooded with stabilizer dispersions at 30 ml/h for 1 PV to optimize foam flooding performance. Foam flooding was conducted subsequently by delivering carbon dioxide gas (90 ml/h) and foam agent solutions (30ml/h) simultaneously into the visual sand pack. The foam was generated in-suit during the co-injection process.

Regarding dynamic experiments in the presence of oil, the sand pack was saturated with crude oil until at least 20 ml of injected oil had been produced. The initial oil saturation was evaluated by mass balance based on the volume of brine produced. Brine flooding

was performed at 30 ml/h and terminated when approximate 98% of water cut was reached. 1 PV of foaming solutions per-flooding at a flow rate of 30 ml/h was conducted similarly with the process of tests without oil. Then carbon dioxide gas (90 ml/h) and foam agent solutions (30ml/h) were co-injected into the core to enable in-suit foam generation.

All the produced fluids (a mixture of crude oil, brine, and/or chemicals including nanoparticles, surfactant, and polymer) were collected with time recorded, and the volume of each fluid was measured to analyze production data.

3.4 Analysis

3.4.1 Static Tests Data Analysis

Normalized Foam Height and Foam Half-life

The normalized foam height is calculated based on the height of foam over the initial foam height, and foam half-life is the time required for the foam to decrease to half of the initial foam height (Singh and Mohanty, 2014).

3.4.2 Dynamic Tests Data Analysis

Permeability Calculation

The permeability, k, the ability of porous rock medium that allows fluids to flow, could be calculated by using Darcy's Law. Darcy's Law for any angle can be written as,

$$q = -\frac{kA}{\mu}\left[\frac{dp}{dl} + \rho g \frac{dz}{dl}\right] \qquad Eqn.1$$

Since all the dynamic experiments were conducted when the sand pack was placed horizontally (z=0), the above equation could be simplified as,

$$q = -\frac{kA}{\mu}\frac{(P_o - P_i)}{L} \qquad Eqn.2$$

By define $m = \frac{kA}{\mu L}$, $Eqn.3$

$$q = -m(P_o - P_i), \qquad Eqn.4$$

$$m = -\frac{q}{P_o - P_i} \qquad Eqn.5$$

where the permeability of the porous medium, k, is in Darcy, L is the length of the sand pack in cm, P_i is the inlet pressure in atm, P_o is the outlet pressure in atm, μ is the fluid viscosity in cp, A is the cross-sectional area of the sand pack in cm^2, and q is the volumetric flow rate in cc/s.

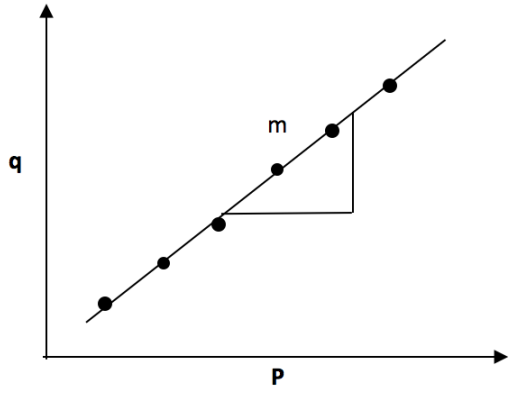

Figure 3.4.2: Slope m in permeability calculation

By using Equation 5, the slope m could be calculated based on the measured experimental data q and P. The permeability measurement was conducted after water saturation. By varying the injection flow rate from 100 cc/hr to 800 cc/hr (increment of 100 cc/hr each time), the corresponding eight pressure drops through the sand pack could be obtained via the pressure transducer. During each pressure difference measurement, one flow rate was required to be maintained at least 20 minutes to ensure the pressure was steady. Once all data required were collected, a plot of flow rate against pressure drops

was carried out, which was illustrated in Figure 3.4.2. And slope m could be simply evaluated.

By knowing the value of slope m, the permeability could be calculated based on the definition of slope m, which was Equation 3,

$$k = \frac{m\mu L}{A} \qquad Eqn. 6$$

All the properties of the porous medium of all the dynamic experiments were listed in Table 3.4.

Experiment	Pore Volume (cc)	Porosity	Length (cm)	Permeability (D)	Initial Oil Saturation
Surfactant	46	36.80%	24.7	7	NA
Surfactant (with oil)	45.5	36.70%	24.5	7.1	90.70%
Surfactant+Nanoparticles	46.2	36.90%	24.7	7.9	NA
Surfactant+Nanoparticles (with oil)	45	36.50%	24.3	7.5	90.80%
Surfactant+Nanoparticles +Polymer	45	36.20%	24.5	7	NA
Surfactant+Nanoparticles+Polymer (with oil)	46	37.10%	24.5	7.9	90.50%
Surfactant+Polymer (with oil)	45.7	37.10%	24.3	7.8	90.20%

Table 3.4: Properties of porous medium of dynamic experiments

Chapter 4: Results and Discussion

4.1 Static Stability of Surfactant-NP System

4.1.1 In the Absence of Oil

The static tests prepared with dispersions of 0.1 wt.% CTAB and 0.1 wt.% CTAB with 1.0 wt.% nanoparticles were conducted. Both of the solutions were in the presence of 0.1 wt.% of sodium chloride. The results of the foam static experiments, including the decays of normalized foam heights, foam half-life values, and foamability were illustrated in Figure 4.1. Compared with the foam generated by the two solutions, the foam generated by surfactant and nanoparticles together exhibited significant favorable stability. By involving nanoparticle into the dispersion, the rates of foam heights decreasing were decelerated dramatically. Foam half-life values, as an important parameter describing foam stability, could be found in the figure as well. The half-life of foam stabilized by surfactant solely was around 10 hours, whereas that of foam created by mixtures of surfactant and nanoparticles was more than 72 hours (experiment ended after 72 hours with a normalized foam height of 0.58). Foamability (initial foam heights) represents the ability of foaming agents to create foam. The combination of surfactant and nanoparticles had better foamability (21% increments), compared with surfactant only case. It could be inferred that synergism had taken place between nanoparticle and surfactants based on the enhanced foam stability and foamability.

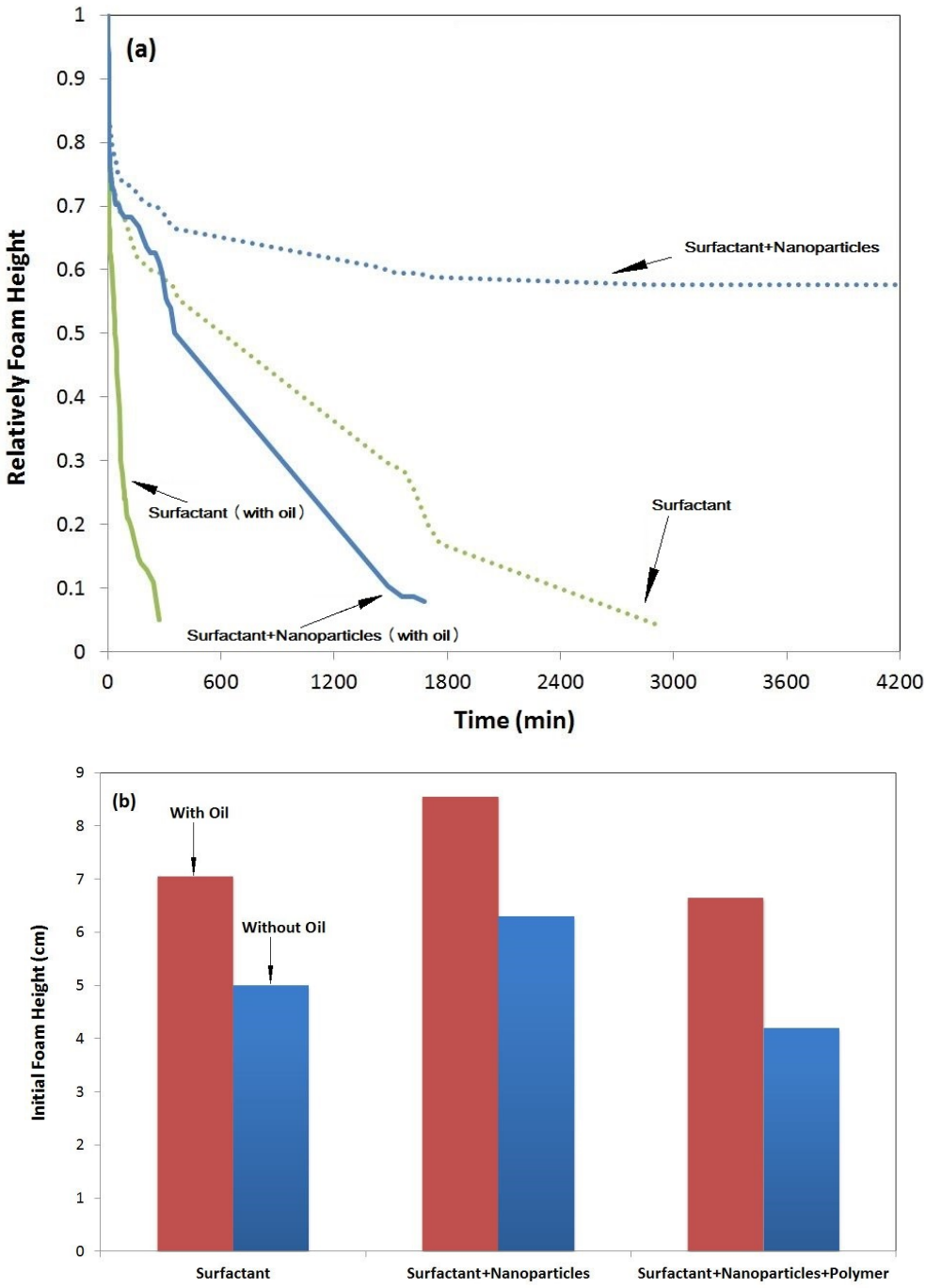

Figure 4.1: (a) Decays of normalized foam heights (b) Initial foam height (foamability) with and without presence of crude oil

4.1.2 In the Presence of Oil

The static experiments were conducted in the presence of oil as well. The heavy oil was added to the surfactant and surfactant with nanoparticles solutions in advance of high-speed homogenization to enable oil to be well dispersed in the foam. Figure 4.1 showed the effects on foam stability and foamability caused by oil addition. Oil tends to act as an antifoam agent, which have a negative impact on foam stability (Koczo et al., 1992). The decays of normalized foam height were accelerated for foam generated with and without nanoparticles. In results, the half-life values reached much earlier for the both cases. The initial foam heights were decreased due to oil introduced as well, representing the shrinkage of foamability. Stability and foamability of surfactant stabilized foam and surfactant-nanoparticle stabilized foam were compared in the presence of oil. Similar to the without oil scenario, foam created by surfactant and nanoparticle was superior in foam stability and foamability, indicating these two foaming agents stabilize foam synergistically. With the help of nanoparticle, foam half-life was improved from 0.6 hours to 5.9 hours, and the whole life of the foam was extended as well.

4.2 Static Stability of Surfactant-NP-Polymer System

Dispersions contained 0.1 wt.% CTAB, 1.0 wt.% nanoparticles, and 500 ppm of polyacrylamide were used to investigate the influence of polymer on foam stability. The results in terms of with and without oil environments were plotted in Figure 4.2. The major function of polymer addition is to enhance the viscosity of aqueous phase. The improved foam stability is due to the declines in both liquid drainage rate and gas diffusion rate between bubbles (Schramm and Kutay, 2000). In terms of polymer addition effect on drain-

age rate, noticeable improvements in drainage rate due to polymer was exhibited in the presence of oil, whereas only slightly difference was observed in the absence of oil. In oil containing foam, the decreases of foam heights over time were mitigated relatively by the polymer, and the half-life values were extended from 5.9 hours to 7.5 hours. Modest enhancements of foam stability were observed in without oil environment. It could be analyzed that polymer addition was able to increase foam stability in some degrees, suggesting SPN foam tends to be more stable compared with foam stabilized by surfactant solely and surfactant-nanoparticle together. Theoretically, foamability diminishes by adding polymers. And the results in both with and without oil scenarios (Figure 4.1) agreed with the theory.

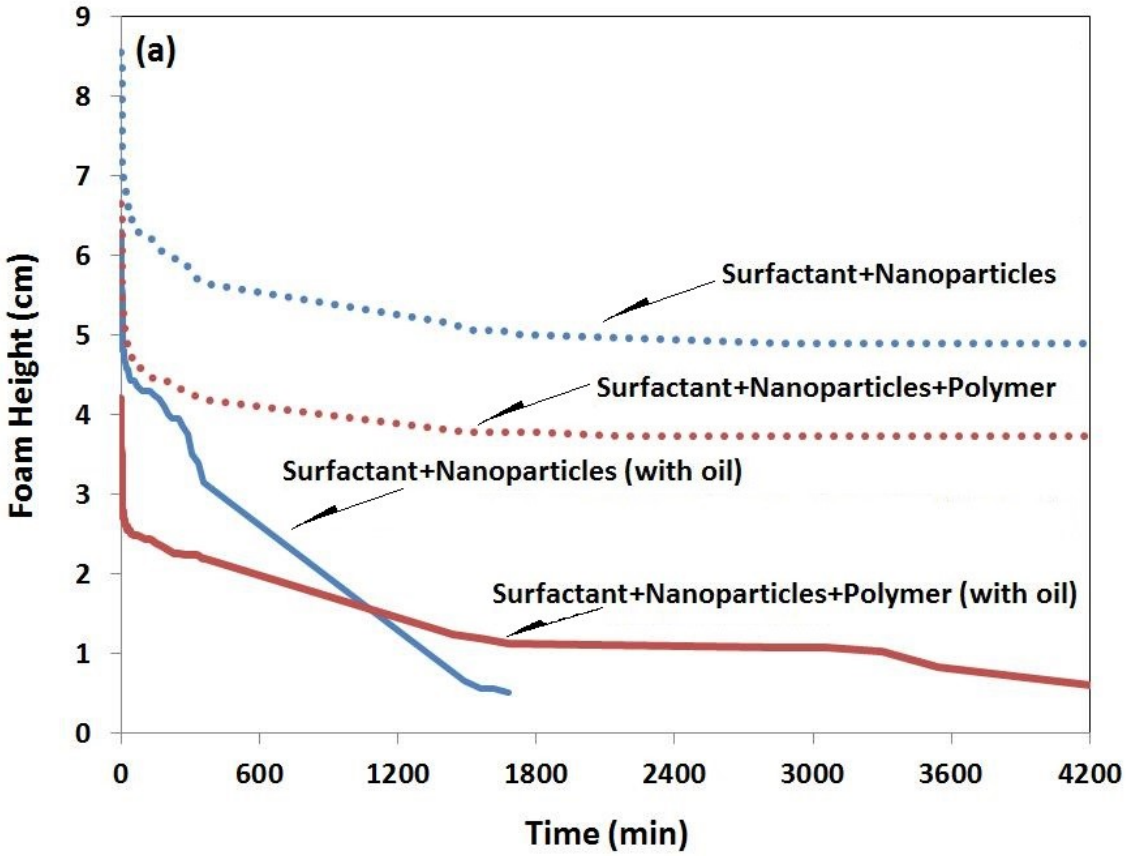
(a)
Foam Height (cm)
Time (min)
Surfactant+Nanoparticles
Surfactant+Nanoparticles+Polymer
Surfactant+Nanoparticles (with oil)
Surfactant+Nanoparticles+Polymer (with oil)
0
1
2
3
4
5
6
7
8
9
0
600
1200
1800
2400
3000
3600
4200

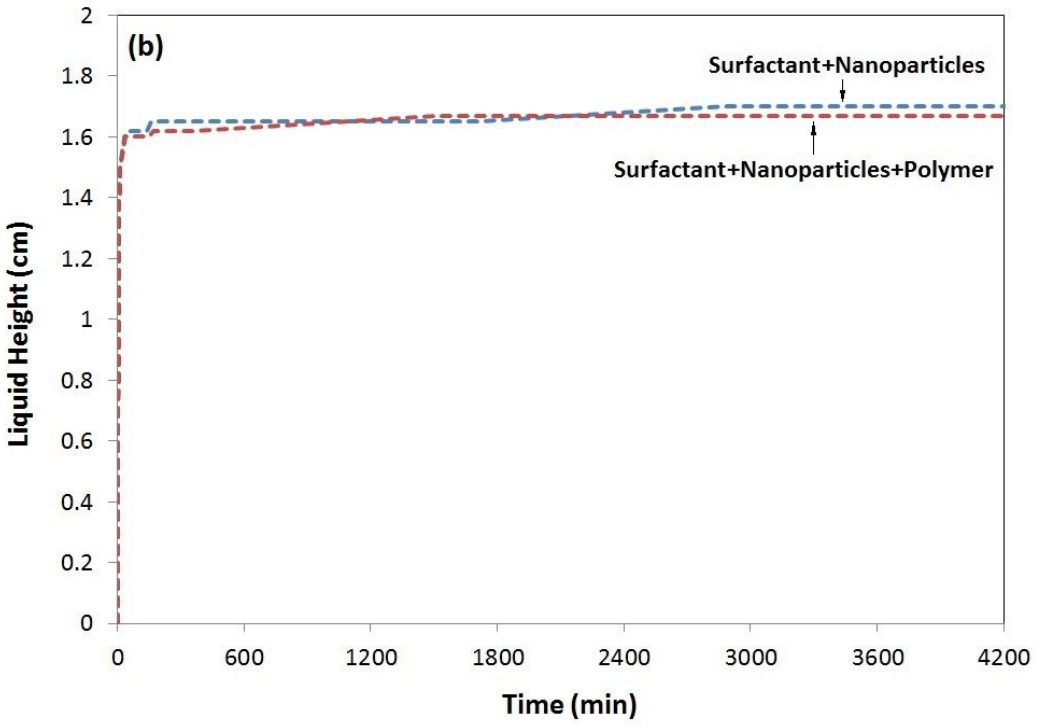

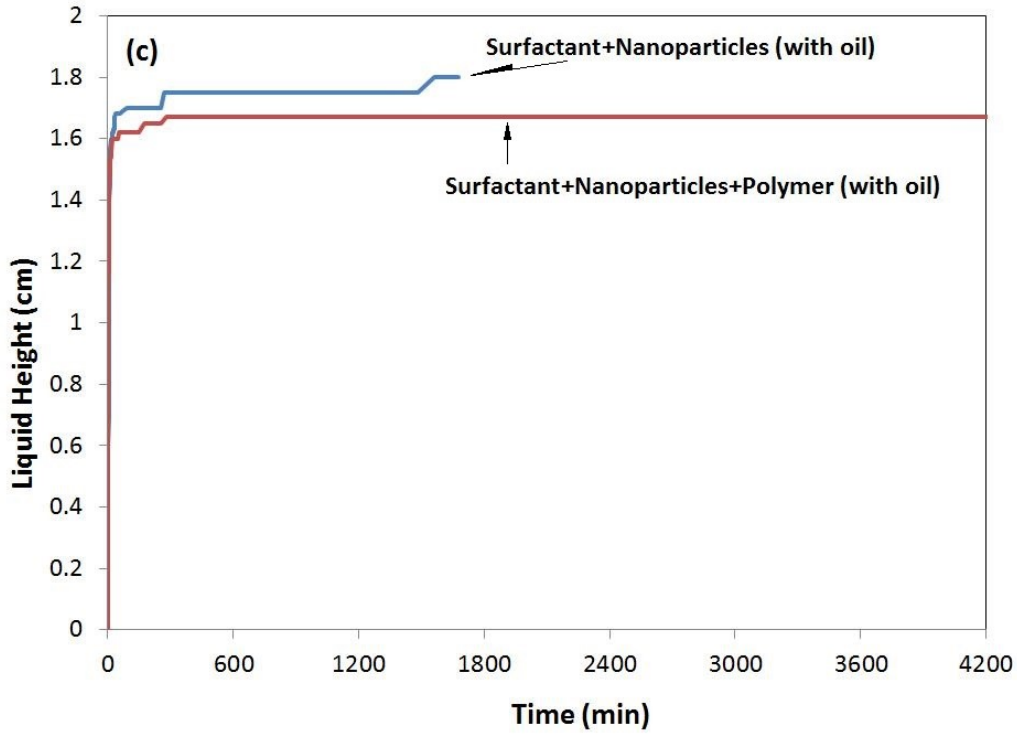

Figure 4.2: (a) Decay of foam height (b) Liquid drainage in the absence of oil (c) Liquid drainage in the presence of oil

4.3 Dynamic Experiments in the Absence of Oil

The dynamic tests discussed in this section were performed in a fully water saturated visual sand pack with three dispersions same as static tests. After 1 PV of foaming dispersions pre-flooding (30 ml/h), foaming solutions and CO_2 gas were co-injected into the cell to in-suit generate foam. With a liquid flow rate of 30 ml/h and gas flow rate of 90ml/h, the foam was created with a quality of 75%. The pressure drops during the 11 PV of foam agent solutions pre-flooding and foam injection were monitored and plotted in Figure 4.3.1. The images of the visual sand pack in foam injection process were shown as well (Figure 4.3.2).

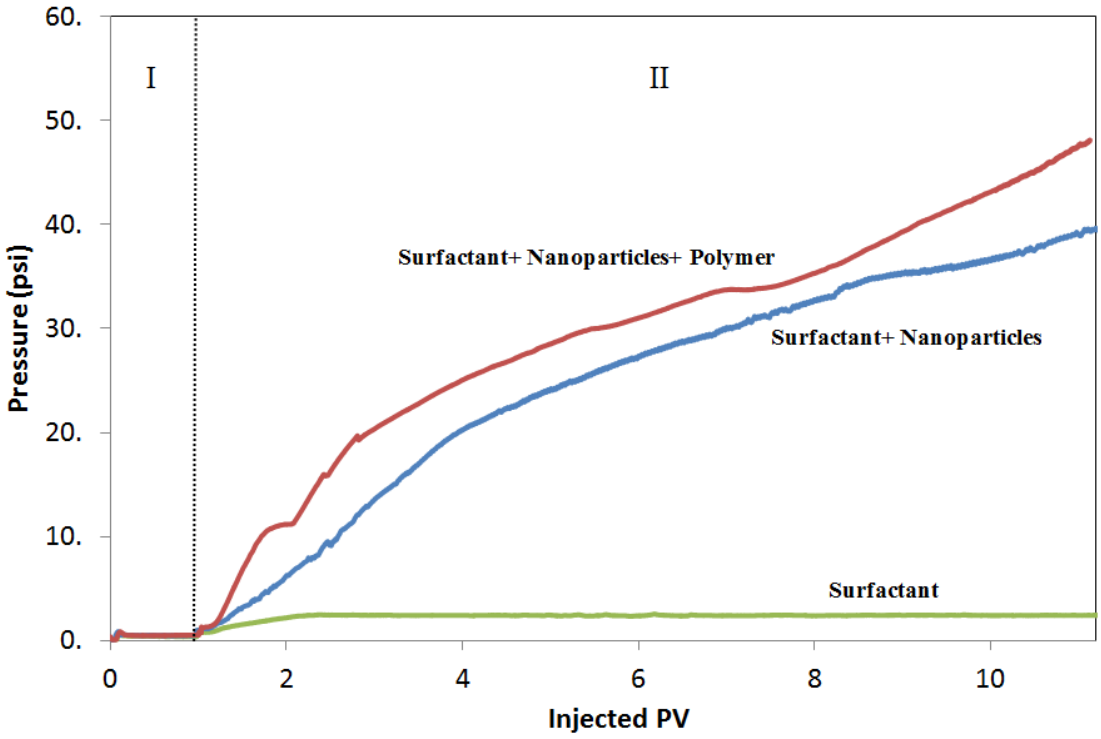

Figure 4.3.1: Pressure profile of foam injection in the absence of crude oil

(Region I: foaming dispersions pre-flushing period; Region II: foam flooding period)

As Figure 4.3.1 illustrated, after 1 PV of foaming solutions injection, foam was created in-suit gradually for all the three dispersions indicated by increments of pressure drops across the porous medium. The rates of pressure drops developed indicated the speed of foam propagation and the relative amounts of pressure differences implied the escalations or diminishments of foam. Based on the pressure profiles, performances of foaming agents could be analyzed. The pressure increasing tendencies of the three dispersions were divergent after foam injections were initiated, which indicated foam propagated differently based on foam stabilizers. Among these foaming solutions, the one consisting of surfactant alone tended to exhibit unfavorable in foam quality and foam escalations, suggested by the relatively low pressure drops. Foam propagated inefficiently and collapsed rapidly through a porous medium, ending with a 2.5 psi pressure difference after 10 PV foam injection. However, the two dispersions with nanoparticles containing achieved extremely desirable performances compared with that of surfactant solely. Foam created by surfactant-nanoparticles blend achieved an obvious increment in pressure drops continually, reaching a pressure difference of 39 psi within the co-injection duration. Foam stabilized by surfactant-nanoparticles-polymer solution developed an improved pressure drops (47 psi) by following the similar pressure increasing tendency with that of the surfactant-nanoparticles blend.

Figure 4.3.2. Foam propagation of surfactant-nanoparticle and surfactant-nanoparticle-polymer tests (the arrow showing as injection direction)

Such inference was evidenced by images captured during the foam injection process (Figure 4.3.2). By dying aqueous phase red, foam or gas could be easily distinguished by being white in color. This satisfying foam propagation was only observed in tests employed stabilizers of surfactant-nanoparticles and surfactant-nanoparticles-polymer. The results revealed that nanoparticles had the ability to enhance foam stability and foamability foam while working synergistically with suitable surfactants, which agreed with results carried out by static tests. With the assistance of polymer, quality of foam could also be enhanced.

4.4 Dynamic Experiments in the Presence of Oil

The dynamic experiments analyzed in this part were conducted in a crude oil saturated sand pack. 3 PV of water was flooded before the foam injection, during what water cut was reached to about 98% and residual oil remained in the visual cell. Foaming disper-

sions were first injected through the core for 1 PV (30 ml/h). Co-injection was then taken place by following the same flow rates and foam quality (75%) performed in the absence of oil condition. Pressure drops (Figure 4.4.1) and oil recoveries (Figure 4.4.2) for foam injection were recorded along with images of the visual sand pack (Figure 4.4.3).

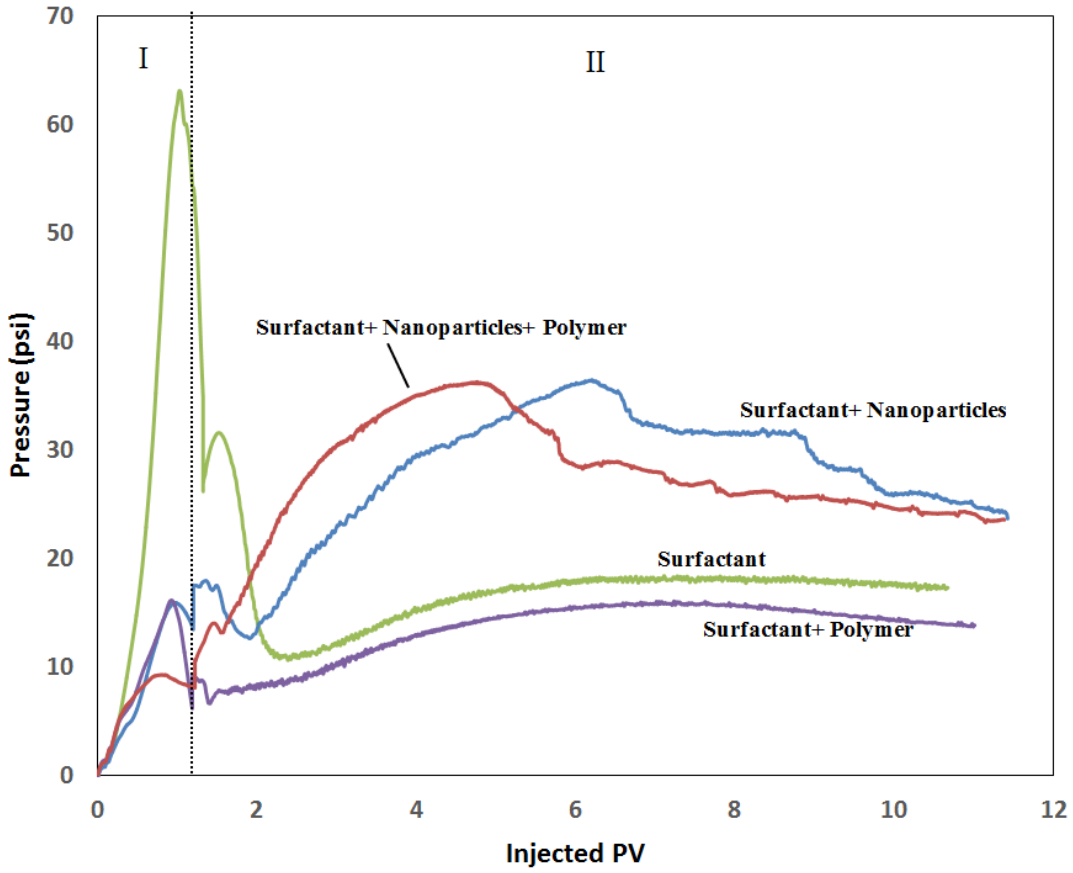

Figure 4.4.1: Pressure profile of foam injection in the presence of crude oil (Region I: foaming dispersions pre-flushing period; Region II: foam flooding period)

According to Figure 4.4.1, the pressure profile consisted of two durations, which were foaming solutions pre-flushing and foam flooding. In terms of foam stabilizers pre-flushing period, disparate foaming dispersions tended to obtain various pressure drops, because different degrees of absorptions and emulsifications took placed in porous mediums based on the natures of foam stabilizers. However, the co-injection (foam flooding) period should be the significant duration need to be focused on. The relative amounts and rates of pressure built up during co-injection demonstrated the efficiency of foam generation and escalations, which were the main criterions used to determine the stability and foamability of a stabilizer. The general tendencies of pressure drops created by different foam agents always started to increase after the initiations of co-injection, implying the formation of foam within the porous medium. Among these combinations of stabilizers, surfactant-nanoparticle and surfactant-nanoparticle-polymer dispersions tended to reach favorable foam flooding performance by comparing the corresponding pressure differences with others. Especially, foam stabilized by surfactant-nanoparticle-polymer mixture built up pressure drops more expeditiously than surfactant-nanoparticle mixture since polymer accelerated the generation of foam. Besides, both of the surfactant and surfactant-polymer dispersions resulted in undesirable foam quality due to the extremely lower pressure drops (more than 20 psi lower than pressure drops created by nanoparticle-containing foam). It suggested that nanoparticle addition contributed to the key factor of foam flooding performance. The synergism between nanoparticle and surfactant obviously improved the foam procreation and polymer posed a positive impact on foam performances as well, which was agreed with the results of the dynamic test in the absence of oil. Additionally, the pressure variations obtained by nanoparticle-

containing foam did not develop as high as pressure differences exhibiting for the dynamic test without oil, because oil generally destabilized foam as discussed in static experiments.

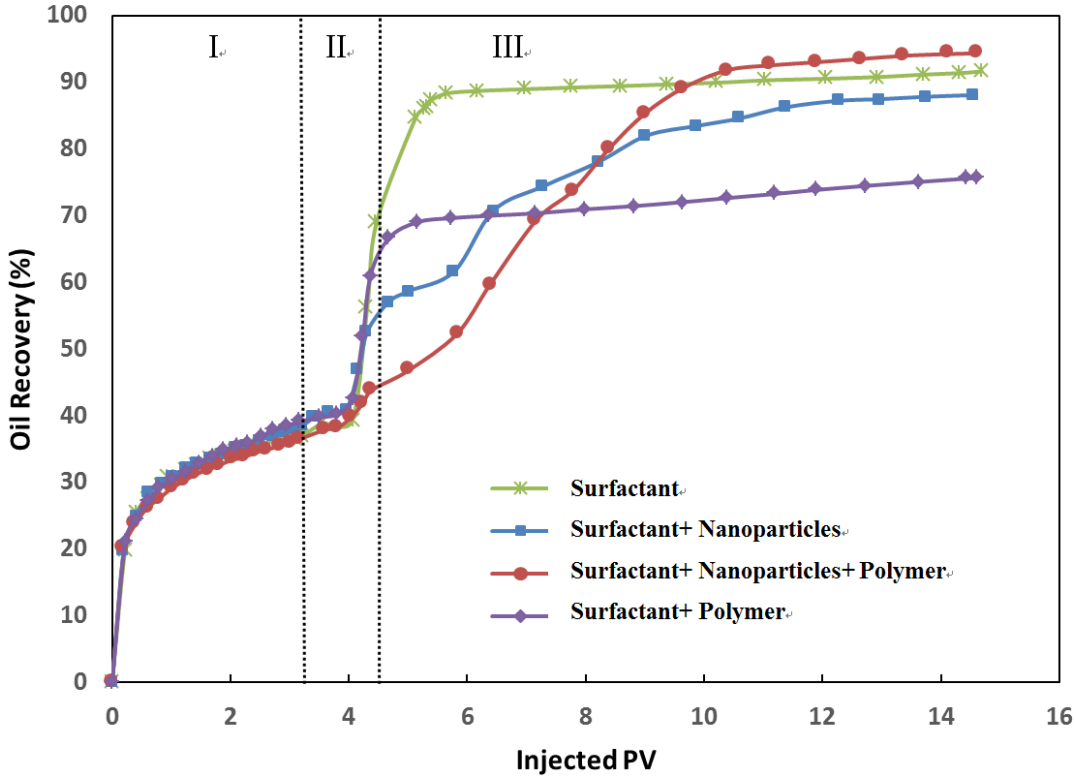

Figure 4.4.2: Oil recovery profile (Region I: water flooding period; Region II: foaming dispersions pre-flushing period; Region III: foam flooding period)

Experiment	Pore Volume (cc)	Porosity	Length (cm)	Permeability (D)	Initial Oil Saturation	Oil Recovery			
						Primary	Secondary	Tertiary	Total
Surfactant	46	36.80%	24.7	7	NA	NA	NA	NA	NA
Surfactant (with oil)	45.5	36.70%	24.5	7.1	90.70%	36.87%	32.10%	22.60%	91.60%
Surfactant+Nanoparticles	46.2	36.90%	24.7	7.9	NA	NA	NA	NA	NA
Surfactant+Nanoparticles (with oil)	45	36.50%	24.3	7.5	90.80%	38.38%	14.30%	35.50%	88.10%
Surfactant+Nanoparticles +Polymer	45	36.20%	24.5	7	NA	NA	NA	NA	NA
Surfactant+Nanoparticles+Polymer (with oil)	46	37.10%	24.5	7.9	90.50%	36.51%	7.40%	50.50%	94.40%
Surfactant+Polymer (with oil)	45.7	37.10%	24.3	7.8	90.20%	39.17%	20.90%	14.60%	75.70%

Table 4.4: Properties of porous medium and oil recoveries of dynamic experiments

As oil recovery profile illustrated (Figure 4.4.2), with similar water flooding recovery, co-injection of surfactant-nanoparticle-polymer blend offered the highest overall oil recovery, followed by that of surfactant, surfactant-nanoparticle, and surfactant-polymer solutions. The unpredicted high surfactant foam recovery was due to the significant increment of pressure drops during per-flushing period. However, when only considering oil recovery of foam flooding period (Table 4.4), surfactant-nanoparticle-polymer foam still gave a preferable oil recovery but followed by surfactant-nanoparticle foam. Surfactant and surfactant-polymer created foam had unsatisfying recovery during co-injection owing to the low quality of foam in the medium. Thus, the results implied that surfactant-nanoparticle-polymer stabilized foam had the ability to sweep most oil among other foams. To curtail expenditures, only surfactant solution could be used for pre-flushing period, no nanoparticle and polymer were necessarily required; however, to optimize foam performance and recovery more oil, nanoparticle along with polymer need to be added for the foam flooding duration.

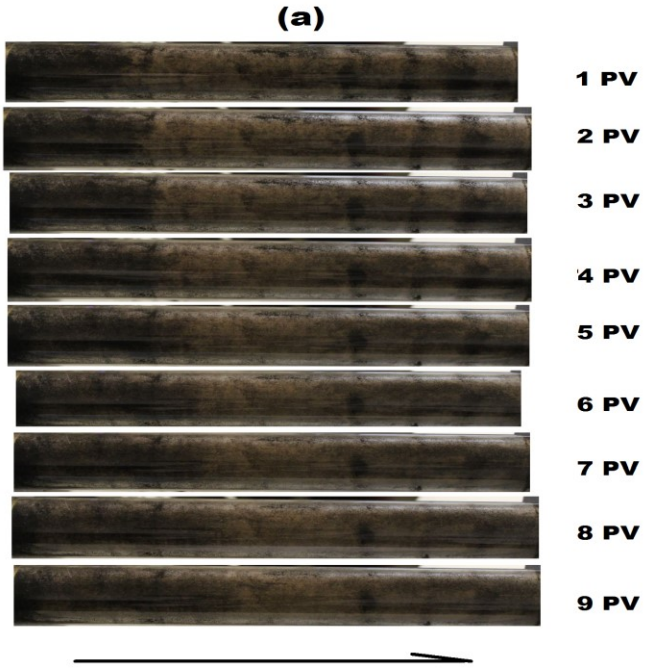
(a)
1 PV
2 PV
3 PV
4 PV
5 PV
6 PV
7 PV
8 PV
9 PV

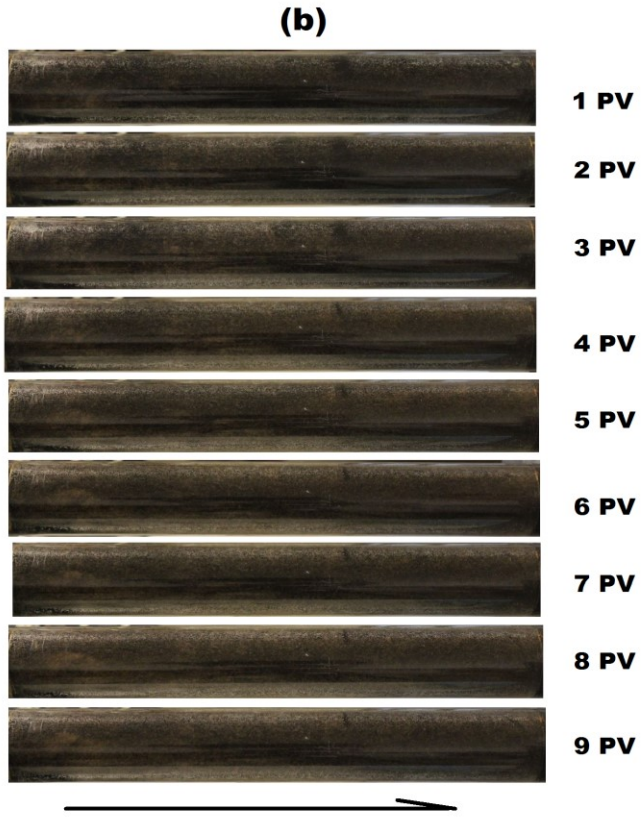
(b)
1 PV
2 PV
3 PV
4 PV
5 PV
6 PV
7 PV
8 PV
9 PV

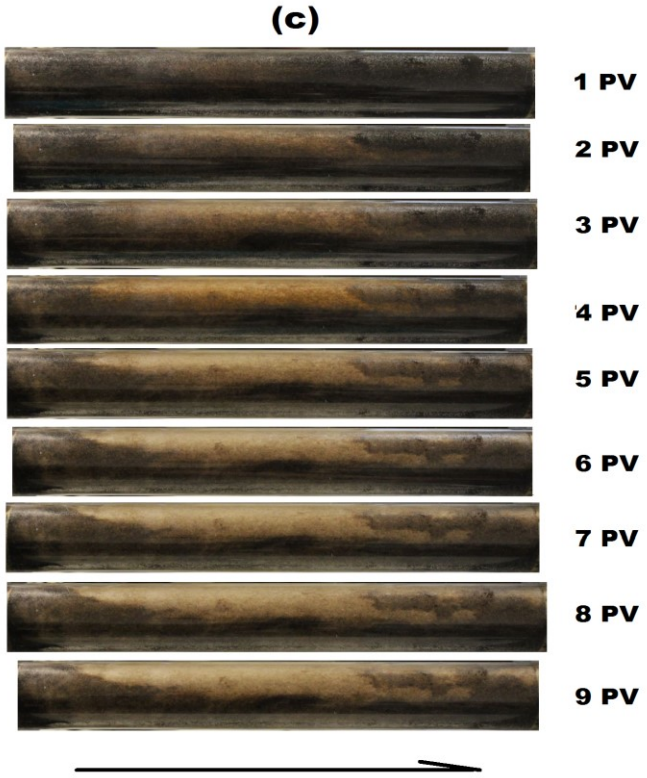
(c)
1 PV
2 PV
3 PV
4 PV
5 PV
6 PV
7 PV
8 PV
9 PV

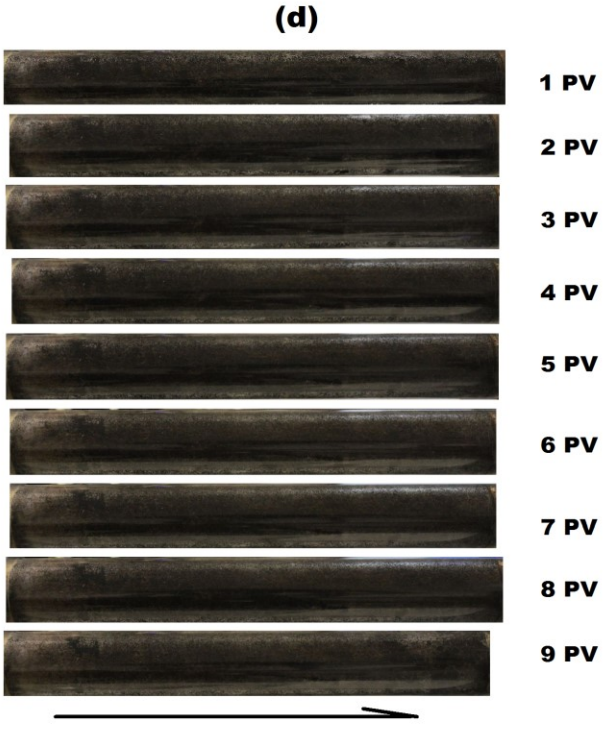
(d)
1 PV
2 PV
3 PV
4 PV
5 PV
6 PV
7 PV
8 PV
9 PV

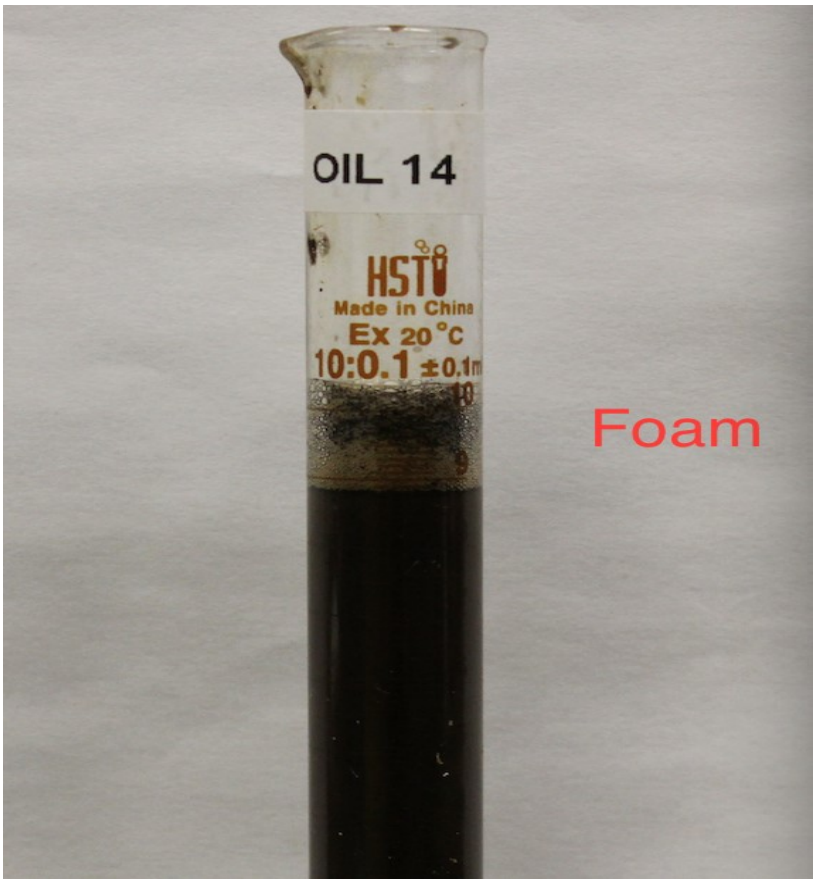

(e)

Figure 4.4.3. Image of visual sand pack during foam injection (the arrow showing as injection direction): (a) Surfactant; (b) Surfactant+Nanoparticles; (c) Surfactant+Nanoparticles +Polymer; (d) Surfactant+ Polymer; (e) Oil sample collected during foam flooding of Surfactant+Nanoparticles +Polymer foam

Chapter 5: Contributions and Recommendations

5.1 Conclusions

Surfactant-nanoparticles foam exhibited superior performances in foam stability and foamability in bulk static tests with and without the presence of crude oil compared to conventional surfactant foam, indicating nanoparticles and surfactants stabilized foam synergistically and efficiently.

Based on static experiments, polymers addition was able to enhance foam stability, and the improvements of foam stability due to polymer addition were more obvious in condition with the presence of heavy oil. And in the meanwhile, polymers tended to diminish foamability.

In water-saturated dynamic experiments, surfactant-nanoparticle dispersion achieved successful foam generation and acceleration, whereas solution with surfactant alone performed unsatisfyingly. Polymer addition affected the foam propagation process positively, resulting in the superior favorable performance of foam stabilized by the surfactant-nanoparticle-polymer blend.

Dynamic tests in the presence of oil implied that foam flooding of surfactant-nanoparticle-polymer blend reached the most desirable pressure drops and overall oil recovery. The synergism between nanoparticle and surfactant apparently enhanced the foam propagations and polymer has a positive impact on foam performances.

5.2 Recommendations for Future Work

- To study foam behaviors under the reservoir conditions, dynamic experiments are recommended to be conducted with high backup pressures, which simulates more likely conditions on field applications. When under high pressure conditions the foam behavior may alter slightly, and results would adapt better in reservoirs.
- In the static experiment, the foam generation was achieved by blending air with a foaming solution. One approachable implementation would be using pure carbon dioxide instead of a mixture of gas sources, which is more convenient to quantify and accurately analyze for better results.
- More data could be analyzed and used to achieve more accurate results if zeta potential is measured. The quantified stability of nanoparticles forming foams can narrow down the range of speculating results thus select preferable fractions of foaming agents' combination.

Reference

Alargova, R. G., Warhadpande, D. S., Paunov, V. N., & Velev, O. D. (2004). Foam superstabilization by polymer microrods. *Langmuir*, **20**(24):10371–10374. http://doi.org/10.1021/la048647a

Bernard, G. G., & Holm, L. W. (1964). Effect of foam on permeability of porous media to gas. *Society of Petroleum Engineers Journal*, **4**(03): 267-274. http://dx.doi.org/10.2118/983-PA

Binks, B. P. (2002). Particles as surfactants—similarities and differences. *Current Opinion in Colloid & Interface Science,* **7**(1–2): 21–41. http://doi.org/10.1016/S1359-0294(02)00008-0

Binks, B. P., Desforges, A., & Duff, D. G. (2007). Synergistic stabilization of emulsions by a mixture of surface-active nanoparticles and surfactant. *Langmuir*, **23**(3): 1098–1106. http://dx.doi.org/10.1021/la062510y

Binks, B. P., & Horozov, T. S. (2005). Aqueous Foams Stabilized Solely by Silica Nanoparticles. *Angewandte Chemie*, **117**(24): 3788–3791. http://dx.doi.org/10.1002/ange.200462470

Binks, B. P., Kirkland, M., & Rodrigues, J. a. (2008). Origin of stabilisation of aqueous foams in nanoparticle–surfactant mixtures. *Soft Matter*, **4**(12*)*: 2373-2382.

http://dx.doi.org/10.1039/b811291f

Binks, B. P., Rodrigues, J. a., & Frith, W. J. (2007). Synergistic interaction in emulsions stabilized by a mixture of silica nanoparticles and cationic surfactant. *Langmuir*, **23**(7): 3626–3636. http://dx.doi.org/10.1021/la0634600

Binks, B. P., & Lumsdon, S. O. (2000). Influence of Particle Wettability on the Type and Stability of Surfactant-Free Emulsions. *Langmuir*, 168622-8631.

Bragg, J.R., and Varadaraj, R. July 17, (2003). Solids-Stabilized Oil –in-Water Emulsion and a Method for Preparing Same, World Intellectual Property Organization, WO 03/057793

Caldelas, F. M. (2010). *Experimental parameter analysis of nanoparticle retention in porous media* (master's thesis). University of Texas at Austin. http://repositories.lib.utexas.edu/handle/2152/ETD-UT-2010-08-2009

Davidson, A. M. (2012). *Magnetic Induction Heating of Superparamagnetic Nanoparticles for Applications in the Energy Industry* (master's thesis). University of Texas at Austin.

Dickson, J. L., Binks, B. P., & Johnston, K. P. (2004). Stabilization of carbon dioxide-in-water emulsions with silica nanoparticles. *Langmuir*, **20**(19): 7976–7983.

http://doi.org/10.1021/la0488102

Eftekhari, A. A., Krastev, R., & Farajzadeh, R. (2015). Foam Stabilized by Fly Ash Nanoparticles for Enhancing Oil Recovery. *Industrial and Engineering Chemistry Research*, **54**(50): 12482–12491. http://doi.org/10.1021/acs.iecr.5b03955

Emrani, A. S., Nasr-el-din, H. A., & Texas, A. (2015). Stabilizing CO2 -Foam using Nanoparticles. In SPE European Formation Damage Conference and Exhibition. Budapest, Hungary, 3–5 June. SPE-174254-MS. http://dx.doi.org/10.2118/174254-MS

Espinosa, D., Caldelas, F., Johnston, K., Bryant, S. L., & Huh, C. (2010). Nanoparticle-Stabilized Supercritical CO 2 Foams for Potential Mobility Control Applications. SPE Improved Oil Recovery Symposium, Tulsa, Oklahoma, USA, 24-28 April. SPE-129925-MS. http://dx.doi.org/10.2118/129925-MS

Gabel, S. T. (2014). *Generation , Stability , and Transport of Nanoparticle-Stabilized Oil-in- Water Emulsions in Porous Media* (master's thesis). University of Texas at Austin.

Koczo, K., Lobo, L. A., & Wasan, D. T. (1992). Effect of oil on foam stability: Aqueous foams stabilized by emulsions. *Journal of Colloid and Interface Science*, **150**(2): 492–506. http://doi.org/10.1016/0021-9797(92)90218-B

Koval, E. J. (1963). A Method for Predicting the Performance of Unstable Miscible Displacement in Heterogeneous Media. *Society of Petroleum Engineers Journal*, **3**(2): 145–154. http://doi.org/10.2118/450-PA

Li, X., Karakashev, S. I., Evans, G. M., & Stevenson, P. (2012). Effect of environmental humidity on static foam stability. *Langmuir : The ACS Journal of Surfaces and Colloids*, **28**(9): 4060–8. http://doi.org/10.1021/la205101d

Lake, L. W., R. T. Johns, W. R. Rossen, and G. A. Pope. 2014. *Fundamentals of Enhanced Oil Recovery*. Society of Petroleum Engineers.

Maestro, A., Rio, E., Drenckhan, W., Langevin, D., & Salonen, A. (2014). Foams stabilised by mixtures of nanoparticles and oppositely charged surfactants: relationship between bubble shrinkage and foam coarsening. *Soft Matter*, **10**(36): 6975–6983. http://doi.org/10.1039/c4sm00047a

Malik, Q. M., & Islam, M. R. (2000). CO2 Injection in the Weyburn Field of Canada: Optimization of Enhanced Oil Recovery and Greenhouse Gas Storage With Horizontal Wells. SPE/DOE Improved Oil Recovery Symposium, Tulsa, Oklahoma, USA, 3-5 April. SPE-59327-MS. http://doi.org/10.2118/59327-MS

McDowell-Boyer, L. M., Hunt, J. R., & Sitar, N. (1986). Particle transport through porous media. *Water Resources Research*, **22**(13): 1901-1921. doi:10.1029/WR022i013p01901

Mo, D., Jia, B., Yu, J., Liu, N., & Lee, R. (2014). Study Nanoparticle-Stabilized CO 2 Foam for Oil Recovery at Different Pressure, Temperature, and Rock Samples. SPE Improved Oil Recovery Symposium, Tulsa, Oklahoma, USA, 12-16 April. SPE-169110-MS. http://doi.org/10.2118/169110-MS

Mungan, N. (1981). Carbon Dioxide Flooding-fundamentals. *Journal of Canadian Petroleum Technology,* **20**(01): 87–92. http://doi.org/10.2118/81-01-03

Nguyen, P., Fadaei, H., & Sinton, D. (2014). Nanoparticle Stablized CO2 in Water Foam for Mobility Control in Enhanced Oil Recovery via Microfluidic Method. SPE Heavy Oil Conference-Canada, Calgary, Alberta, Canada, 10-12 June. SPE-170167-MS. http://dx.doi.org/10.2118/170167-MS

Paul, K. T., Satpathy, S. K., Manna, I., Chakraborty, K. K., & Nando, G. B. (2007). Preparation and Characterization of Nano structured Materials from Fly Ash: A Waste from Thermal Power Stations, by High Energy Ball Milling. *Nanoscale Research Letters*, **2**(8): 397–404. http://dx.doi.org/10.1007/s11671-007-9074-4

Roberts, M. R. (2011). *Shear-Induced Emulsions Stabilized with Surface-Modified Silica Nanoparticles.* MS thesis, The University of Texas at Austin, Austin, Texas, USA (May 2011)

Rodriguez, E., Roberts, M. R., Yu, H., Huh, C., & Bryant, S. L. (2009). SPE 124418 Enhanced Migration of Surface-Treated Nanoparticles in Sedimentary Rocks. S*PE Annual Technical Conference And Exhibition*, 42058-2078.

Rossen, W., van Duijn, C., Nguyen, Q., Shen, C., & Vikingstad, A. (2010). Injection strategies to overcome gravity segregation in simultaneous gas and water injection into homogeneous reservoirs. *SPE Journal*, **15**(01): 76–90. http://dx.doi.org/10.2118/99794-PA

Schramm, L. L., & Kutay, S. M. (2000). Structure / Performance Relationships for Surfactant Stabilized Foams in Porous Media. Canadian International Petroleum Conference, Calgary, Alberta, 4-8 June. PETSOC-2000-064. http://doi.org/10.2118/2000-064

Singh, R., & Mohanty, K. K. (2014). Foams Stabilized by In-Situ Surface Activated Nanoparticles in Bulk and Porous Media. *SPE Annual Technical Conference and Exhibition.* http://doi.org/10.2118/170942-MS

Singh, R., & Mohanty, K. K. (2014). Synergistic Stabilization of Foams by a Mixture of Nanoparticles and Surfactants. SPE Improved Oil Recovery Symposium, Tulsa, Oklahoma, USA, 12-16 April. SPE-169126-MS. http://doi.org/10.2118/169126-MS

Singh, R., & Mohanty, K. K. (2015). Foams Stabilized by In-Situ Surface- Activated Nanoparticles in Bulk and Porous Media. *SPE Journal*. SPE-170942-PA (in press; posted March 2015).

Sun, Q., Li, Z., Wang, J., Li, S., Li, B., Jiang, L., … Liu, W. (2015). Aqueous Foam Stabilized by Partially Hydrophobic Nanoparticles in the Presence of Surfactant. *Colloids and Surfaces A: Physicochemical and Engineering Aspects* **471**: 54–64. http://doi.org/10.1016/j.colsurfa.2015.02.007

Sydansk, R. D. (1994). Polymer-Enhanced Foams Part 1: Laboratory Development And Evaluation. *SPE Advanced Technology Series* **2**(02): 150-159. SPE-25168-PA.

Telmadarreie, A., Trivedi, J.J., (2016). New Insight on Carbonate-Heavy-Oil Recovery: Pore-Scale Mechanisms of Post-Solvent Carbon Dioxide Foam/Polymer-Enhanced-Foam Flooding. *SPE Journal*. SPE-174510-PA, http://dx.doi.org/10.2118/174510-PA

Thomas, A., Gaillard, N., & Favero, C. (2012). Some Key Features to Consider When Studying Acrylamide-Based Polymers for Chemical Enhanced Oil Recovery. *Oil and Gas Science and Technology*, **67**(6): 887–902. http://dx.doi.org/10.2516/ogst2012065

Worthen, A. J., Bagaria, H. G., Chen, Y., Bryant, S. L., Huh, C., & Johnston, K. P. (2013). Nanoparticle-stabilized carbon dioxide-in-water foams with fine texture. *Journal of Colloid and Interface Science*, **391**: 142–51. http://doi.org/10.1016/j.jcis.2012.09.043

Worthen, A., Bagaria, H., Chen, Y., Bryant, S. L., Huh, C., & Johnston, K. P. (2012). Nanoparticle Stabilized Carbon Dioxide in Water Foams for Enhanced Oil Recovery. *Society of Petroleum Engineers. doi:10.2118/154285-MS*

Yu, J., Liu, N., Li, L., & Lee, R. (2012). Generation of Nanoparticle-Stabilized Supercritical CO2 Foams. Carbon Management Technology Conference, Orlando, Florida, USA, 7-9 February. CMTC-150849-MS. http://dx.doi.org/10.7122/150849-MS

Zhang, T., et al. (2011). Engineered Nanoparticles as Harsh-Condition Emulsion and Foam Stabilizers and as Novel Sensors. *Offshore Technology Conference; Offshore Technology Conference -Cd-Rom Edition-*, OTC21212.

Zhang, T., Roberts, M. R., Bryant, S. L., & Huh, C. (2009). Foams and Emulsions Stabilized With Nanoparticles for Potential Conformance Control Applications. *Spe International Symposium On Oilfield Chemistry*, 21024-1040.

Zhang, T., Davidson, A., Bryant, S. L., & Huh, C. (2010). SPE 129885: Nanoparticle-Stabilized Emulsions for Applications in Enhanced Oil Recovery. *Spe/Doe Symposium On Improved Oil Recovery,* 21009-1026.

Zhou, X., Han, M., Fuseni, A. B., & Yousef, A. A. (2012). SPE 153988 Adsorption-Desorption of an Amphoteric Surfactant onto Permeable Carbonate Rocks. *Spe/Doe Symposium On Improved Oil Recovery*, 1552-57